NEW PARADIGMS FOR THE ANALYSIS OF AD HOC NETWORKS

A Proposal

Submitted to the Graduate School

of the University of Notre Dame

in Partial Fulfillment of the Requirements

for the Degree of

Doctor of Philosophy

in

Electrical Engineering

by

Sunil Srinivasa,  B. Tech., M.S.

_____

Martin Haenggi, Director

Graduate Program in Electrical Engineering

Notre Dame, Indiana

March 2009

NEW PARADIGMS FOR THE ANALYSIS OF AD HOC NETWORKS

Abstract

by

Sunil Srinivasa

This proposal introduces two new paradigms that help simplify the analysis of ad hoc networks:

First, we use concepts from stochastic geometry to analytically determine the distribution of internode distances in a finite uniformly random network. The key finding is that when a known number of nodes are uniformly randomly placed inside a ball of arbitrary dimensions, the probability density function of the internode distances follows a generalized beta distribution. This result is applied to study important single-hop characteristics of ad hoc networks such as interference, outage and connectivity.

Second, we consider a multihop wireless line network with a single unidirectional data flow. We show that by simply limiting the buffer sizes at the relay nodes to unity and making minor amendments to the MAC protocol, the flow of traffic in the network can be efficiently regulated in a completely distributed fashion. Upon employing this revised transmission policy, we observe that the transport of packets in the system is analogous to the flow of particles in the totally asymmetric simple exclusion process. Using existing results from statistical mechanics, we analytically characterize the end-to-end delay and throughput performance of multihop wireless networks at steady state for two different channel access schemes and provide applications of our findings for large wireless line networks.

Proposed research goals are to characterize the delay and throughput performance in a system of networks and to design appropriate routing protocols and network architectures that optimize the system performance. Additional objectives are to study the throughput-delay-reliability tradeoffs and to understand the transient behavior of wireless line networks.

CONTENTS

CHAPTER 1

INTRODUCTION

The past few years have witnessed a surge of revolutionary research developments in the area of wireless communications and networking. Notable contributions include the near-capacity-achieving LDPC and turbo codes, which have now become a standard in the developing market for highly efficient transmission schemes, and technical breakthroughs such as CDMA, MIMO, and OFDM that have brought completely new perspectives on how to intelligently communicate over wireless channels. Such advances in information theory and communication theory have significantly helped further wireless systems' performance in a very short span of time and have provided the thrust for the rapid evolvement of high-rate data communication. However, inherent difficulties have stunted our progress from the era of tetherless connectivity predominated by centralized cellular networks and WLANs to the era of ubiquitous wireless connectivity predominated by decentralized ad hoc networks [1].

First, while classical information theory has been extremely successful for studying point-to-multipoint links, it is not yet developed enough to characterize the intricacies of multipoint-to-multipoint networks that arise due to the inherent interactions between nodes. In fact, the capacity of a general relay channel with just three nodes is still an open problem. Second, due to the multihop nature of data communication in an ad hoc network, the flows across various links are spatially and temporally correlated and this fact needs to be explicitly considered during their analysis and design. Queueing theory has proven to be particularly useful in this regard, but the analysis gets very cumbersome as the network size grows. Third, in order to optimize the performance of ad hoc networks, a cross-layer design needs to be adopted wherein the interdependencies among the layers of the protocol stack must be taken into account [2]. Furthermore, the design approach needs to be adaptive to changes in the system and thus is quite a

challenging task. Owing to such barriers, the performance of general ad hoc networks has not yet been quantified, and optimal ways of designing and operating them are known only for a few specific and/or oversimplified cases.

In view of these difficulties, researchers are turning to other branches of study to obtain ideas and methodologies that help better understand and characterize the dynamical behavior of wireless networks. Of late, statistical physics has, in particular, captured the attention of the research community since it contains a rich collection of mathematical tools and methodologies for studying interacting many-particle systems. Statistical physics methodologies such as the mean field theory has been successfully applied to study coding over multiuser MIMO channels [3, 4]. In [5], the authors use ideas such as the replica method to characterize the performance of multiuser detection in CDMA. The statistical mechanics of interfering transmissions in wireless networks has been studied in [6]. Tools from statistical physics have also been successfully applied to study interesting problems in random communication networks such as percolation, connectivity and capacity [7]. Using analogous concepts from other subject areas has considerably enhanced our understanding of wireless networks and has helped further the research in the ad hoc networking community.

On similar lines, our work introduces two new paradigms that help simplify the analysis and design of ad hoc networks:

First we use concepts from stochastic geometry to analytically determine the distribution of internode distances in a finite uniformly random network. This is then applied to study important single-hop characteristics of ad hoc networks such as interference, outage, connectivity, energy consumption and routing.

Second, we apply some results from the Totally Asymmetric Simple Exclusion Process (TASEP), a simple model in statistical mechanics describing particle flow in an interacting system, to characterize the throughput and delay performance of multi-hop wireless line networks.

The detailed organization of the proposal is as follows.

Chapter 2 deals with the theory and applications of internode distance distributions in random wireless networks. When determining distance distributions in random networks, the underlying nodal arrangement is almost universally taken to be a stationary

Poisson point process. While this may be a good approximation in some cases, there are also certain shortcomings to this model such as the fact that in practical networks, the number of nodes in disjoint areas are not independent. This chapter considers a more realistic network model where a known and fixed number of nodes are independently distributed in a given region and characterizes the distribution of the Euclidean internode distances. The key finding is that when the nodes are uniformly randomly placed inside a ball of arbitrary dimensions, the probability density function of the internode distances follows a generalized beta distribution. This result is applied to study single-hop wireless network characteristics such as energy consumption, interference, outage and connectivity.

In Chapter 3, we consider a multihop wireless line network with a single unidirectional data flow. We show that by simply limiting the buffer sizes at the relay nodes to unity and making minor amendments to the MAC protocol, the flow of traffic in the network can be efficiently regulated in a completely distributed fashion. Upon employing this revised transmission policy, we observe that the transport of packets in the system is analogous to the flow of particles in the totally asymmetric simple exclusion process (TASEP). Using existing results from statistical mechanics, we characterize the end-to-end delay and throughput performance of multihop wireless networks at steady state for two different channel access schemes. Additionally, we study the spatial correlations involved between the delays across different hops and provide applications of our findings for large wireless line networks. This work also aims at promoting the TASEP as a powerful tool for analyzing the performance of wireless networks.

Chapter 4 describes the proposed future work and discusses several interesting open questions. The basic research goals are to analytically characterize (or at least provide upper and lower bounds to) the delay and throughput performance in a system of multihop wireless networks, and to design appropriate routing protocols and network architectures that optimize the system performance. Additional objectives are to study the throughput-delay-reliability tradeoffs in multihop line networks and to understand their transient behavior, which refers to the dynamics of the network before it reaches steady state.

CHAPTER 2

DISTANCE DISTRIBUTIONS IN FINITE UNIFORMLY RANDOM NETWORKS:
THEORY AND APPLICATIONS

2.1   Introduction

2.1.1   Motivation

In wireless channels, the received signal strength falls off with distance according to

a power law, at a rate termed the large scale path loss exponent (PLE) [8]. Given a link

distance $l$, the signal power at the receiver is attenuated by a factor of $l^{-\alpha}$, where $\alpha$ is

the PLE. Consequently, in wireless networks, distances between nodes strongly impact

the signal-to-noise-and-interference ratios (SINRs), and, in turn, the link reliabilities.

The knowledge of the nodal distances is therefore essential for the performance analysis

and the design of efficient protocols and algorithms.

In many wireless networks, nodes can be assumed to be scattered randomly over

an area or volume; the distance distributions then follow from the spatial stochastic

process governing the locations of the nodes. For the sake of analytical convenience, the

arrangement of nodes in a random network is commonly taken to be a homogeneous (or

stationary) Poisson point process (PPP). For the resulting so-called "Poisson network"

of density $\lambda$, the number of nodes in any given set $V$ of Lebesgue measure $|V|$ is Poisson

with mean $\lambda|V|$, and the numbers of nodes in disjoint sets are independent. Even though

the PPP model is a good approximation when the network density is known, and can

lead to some insightful results, practical networks differ from Poisson networks in certain

aspects. First, networks are usually formed by scattering a fixed (and finite) number of

nodes in a given area. In this case, the nodal arrangement is a *binomial point process*

(BPP), which we define shortly. Secondly, since the area or volume of deployment is

necessarily finite, the point process formed is non-stationary and often non-isotropic,

meaning that the network characteristics as seen from a node's perspective such as the

4

nearest-neighbor distance or the interference distribution is not the same for all nodes. Furthermore, the numbers of nodes in disjoint sets are not independent; in the case of the BPP, they are governed by a multinomial distribution.

**Definition 2.1.1.** *Formally, a BPP $\Phi$ is formed as a result of distributing $N$ points independently uniformly in a compact set $W$.*

The density of the BPP at any location $x$ is defined to be $\lambda(x) = \frac{N}{|W|}\mathbf{1}_W(x)$, where $\mathbf{1}$ denotes the indicator function. In this work, we consider $W \subset \mathbb{R}^d$ ($d$ is an arbitrary positive integer). For any set $V \subset \mathbb{R}^d$, the number of points in $V$, $\Phi(V)$, is binomial$(n, p)$ with parameters $n = N$ and $p = |V \cap W|/|W|$ [9]. By this property, the number of nodes in disjoint sets are joint via a multinomial distribution. Accordingly, for disjoint sets $V_1, \ldots, V_k$ and $n = n_1 + \ldots + n_k$, we have

$$\Pr(\Phi(V_1) = n_1, \ldots, \Phi(V_k) = n_k) = \frac{n!}{n_1! \cdots n_k!} \frac{|V_1 \cap W|^{n_1} \cdots |V_k \cap W|^{n_k}}{|W|^n}.$$

If the number of nodes or users is known, the PPP is clearly not a good model, since realizations of the process may have more nodes than the number of nodes deployed or no nodes at all. In particular when the number of nodes is small, the Poisson model is inaccurate. The main shortcoming of the Poisson assumption is, however, the independence of the number of nodes in disjoint areas. For example, if all the $N$ nodes are located in a certain part of the network area, the remaining area is necessarily empty. This simple fact is not captured by the Poisson model. This motivates the need to study and accurately characterize finite uniformly random networks, in an attempt to extend the plethora of results for the PPP to the often more realistic case of the BPP. We call this new model a *binomial network*, and it applies to mobile ad hoc and sensor networks and wireless networks with infrastructure, such as cellular telephony networks.

In this work, we analytically characterize the distribution of internode distances in a binomial network wherein a known number of nodes are independently distributed in a compact set. As a special case, we derive the Euclidean distance properties in a $d$-dimensional isotropic[1] BPP, and use it to study relevant problems in wireless networks such as energy consumption, design of efficient forwarding and localization algorithms, interference characterization, and outage and connection probability evaluation.

---

[1] A point process is said to be isotropic if its distribution is invariant to rotations.

### 2.1.2 Related Work

Even though the knowledge of the statistics of the node locations in wireless networks is crucial, relatively few results are available in the literature in this area. Moreover, much of the existing work deals only with first and perhaps second moments of the distances (means and variances) or characterizes the exact distribution only for very specific system models.

In [10], the probability density function (pdf) and cumulative distribution function (cdf) of the distances between two randomly chosen nodes are derived for networks with uniformly random and Gaussian distributed nodes over a rectangular area. [11] studies mean internodal distance properties for several kinds of multihop systems such as ring networks, Manhattan street networks, hypercubes and shufflenets. [12] provides closed-form expressions for the distributions in $d$-dimensional homogeneous PPPs and describes several applications of the results for large networks. [13] considers one-dimensional Poisson networks and analyzes the distribution and moments of the single-hop distance, which is defined as the maximum possible distance between two nodes that can communicate with each other. [14] derives the joint distribution of distances of nodes from a common reference point for networks with a finite number of nodes randomly distributed on a square and [15] determines the pdf and cdf of the distance between two randomly selected nodes in square random networks.

### 2.2 Distribution of Internode Distances

In this section, we determine the distribution of the Euclidean distance to the $n^{\text{th}}$ nearest point from an arbitrary reference point for a general BPP. In the special case of a $d$-dimensional isotropic BPP, we establish that this random variable (r.v.) follows a generalized beta distribution. We also derive the distances to the nearest and farthest nodes and the void probabilities.

Consider the BPP $\Phi$ with $N$ points uniformly randomly distributed in a compact set $W \subset \mathbb{R}^d$ (see Fig. 2.1). Let $R_n$ denote the r.v. representing the Euclidean distance from an arbitrary reference point $x$ to the $n^{\text{th}}$ nearest node of the BPP[2] and let $b_d(x, r)$ denote the $d$-dimensional ball of radius $r$ centered at $x$.

---

[2]For the rest of the chapter, we assume that $x$ is not a point of the BPP. However, if $x \in \Phi$, the remaining point process simply becomes a BPP with $N - 1$ points.
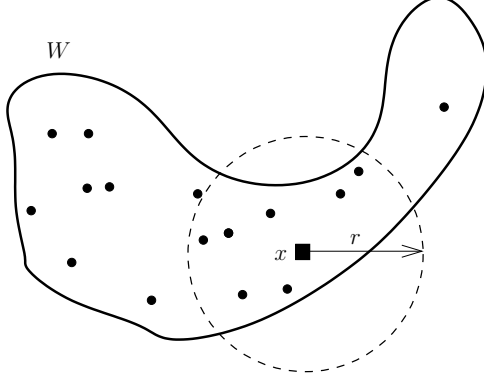
Figure 2.1. A BPP with $N = 16$ points uniformly randomly distributed in an arbitrary compact set $W$. We wish to determine the distribution of the distances to the other points from the reference point $x$. The dashed circle represents the ball $b_d(x, r)$.

The complementary cumulative distribution function (ccdf) of $R_n$ is the probability that there are less than $n$ points in $b_d(x, r)$ :

$$\bar{F}_{R_n}(r) = \sum_{k=0}^{n-1} \binom{N}{k} p^k (1-p)^{N-k}, \quad 0 \leq r \leq R, \tag{2.1}$$

where $p = |b_d(x, r) \cap W| / |W|$. In the case of a *non-homogeneous* BPP with a general density function $\lambda(x)$, $p = \int_{b_d(x,r) \cap W} \lambda(x) \mathrm{d}x$.

$\bar{F}_{R_n}$ can be written in terms of the regularized incomplete beta function as

$$\bar{F}_{R_n}(r) = I_{1-p}(N - n + 1, n), \quad 0 \leq r \leq R, \tag{2.2}$$

where

$$I_x(a, b) = \frac{\int_0^x t^{a-1}(1-t)^{b-1}\mathrm{d}t}{B(a, b)}.$$

Here, $B(a, b)$ denotes the beta function, which is expressible in terms of gamma functions as $B(a, b) = \Gamma(a)\Gamma(b)/\Gamma(a + b)$.

The pdf of the distance function is given by

$$\begin{aligned} f_{R_n} &= -\mathrm{d}\bar{F}_{R_n}/\mathrm{d}r \\ &= \frac{\mathrm{d}p}{\mathrm{d}r} \frac{(1-p)^{N-n} p^{n-1}}{B(N - n + 1, n)}. \end{aligned} \tag{2.3}$$

We now analytically derive the pdf of the Euclidean distance between points in a $d$-dimensional isotropic BPP, and later, in Section 2.3, compute its moments. In Section 2.4, we derive the pdf of the distances when $W$ is a general $l$-sided regular polygon. In Section 2.5, we apply our findings to the study of wireless networks.

7

**Theorem 2.2.1.** *In a point process consisting of $N$ points uniformly randomly distributed in a $d$-dimensional ball of radius $R$ centered at the origin, the Euclidean distance $R_n$ from the origin to its $n^{th}$ nearest point follows a generalized beta distribution, i.e.,*

$$f_{R_n}(r) = \frac{d}{R} \frac{B(n-1/d+1, N-n+1)}{B(N-n+1, n)} \beta\left( \left(\frac{r}{R}\right)^d ; n - \frac{1}{d} + 1, N - n + 1 \right), \quad r \in [0, R],$$

*where $\beta(x; a, b)$ is the beta density function[3] defined as $\beta(x; a, b) = \frac{1}{B(a,b)} x^{a-1}(1-x)^{b-1}$.*

*Proof:* For the isotropic $d$-dimensional BPP, we have $W = b_d(o, R)$ where $o$ represents the origin. The volume of this ball $|W|$ is equal to $c_d R^d$, where

$$c_d = |b_d(o, 1)| = \frac{\pi^{d/2}}{\Gamma(1 + d/2)}$$

is the volume of the unit ball in $\mathbb{R}^d$ [9]. Important cases include $c_1 = 2$, $c_2 = \pi$ and $c_3 = 4\pi/3$. The density of this process is equal to $N/(c_d R^d)$ inside the ball.

With the reference point being the origin, note that $p = c_d r^d / c_d R^d = (r/R)^d$ and from (2.3), we have

$$
\begin{aligned}
f_{R_n}(r) &= \frac{d}{R} \left(\frac{r}{R}\right)^{d-1} \frac{(1-p)^{N-n} p^{n-1}}{B(N-n+1, n)} \\
&= \frac{d}{R} \frac{(1-p)^{N-n} p^{n-1/d}}{B(N-n+1, n)} \\
&= \frac{d}{R} \frac{B(n-1/d+1, N-n+1)}{B(N-n+1, n)} \beta\left( \left(\frac{r}{R}\right)^d ; n - \frac{1}{d} + 1, N - n + 1 \right) \quad (2.4)
\end{aligned}
$$

for $0 \leq r \leq R$. The final equality casts $R_n$ as a generalized beta-distributed variable.

$\square$

**Corollary 2.2.2.** *For the practical cases of $d = 1$ and $d = 2$, we have*

$$f_{R_n}(r) = \frac{1}{R} \beta\left(\frac{r}{R}; n, N - n + 1\right)$$

*and*

$$f_{R_n}(r) = \frac{2}{R} \frac{\Gamma(n + \frac{1}{2})\Gamma(N + 1)}{\Gamma(n)\Gamma(N + \frac{3}{2})} \beta\left(\frac{r^2}{R^2}; n + \frac{1}{2}, N - n + 1\right)$$

*respectively.*

Fig. 2.2 plots the distance pdfs for the cases of $d = 1$ and $d = 2$.

Remarks:

1. The void probability $p_B^0$ of the point process is defined as the probability of there being no point of the process in an arbitrary test set $B$ [9]. For a BPP with $N$ points distributed over a set $W$, it is easy to see that

$$p_B^0 = (1 - |B \cap W|/|W|)^N. \quad (2.5)$$

---

[3]Mathematica: PDF[BetaDistribution[a, b],x].

8

For the isotropic BPP considered above, when the test set is $B = b_d(o, r)$, we have
$p_B^0 = \left(1 - (r/R)^d\right)^N$.

2. Of interest in particular are the nearest- and farthest-node distances. The nearest-node distance pdf is given by

$$f_{R_1}(r) = \frac{dN}{r}\left(1 - \left(\frac{r}{R}\right)^d\right)^{N-1}\left(\frac{r}{R}\right)^d, \tag{2.6}$$

and the distance to the farthest point from the origin is distributed as

$$f_{R_N}(r) = \frac{dN}{r}\left(\frac{r}{R}\right)^{Nd}, \quad 0 \le r \le R. \tag{2.7}$$

Both are generalized Kumaraswamy distributions [16].

3. For a one-dimensional BPP, $f_{R_n}(r) = f_{R_{N-n+1}}(R - r)$, and therefore knowledge of the distance pdfs for the nearest $\lceil N/2 \rceil$ nodes gives complete information on the distance distributions to the other points.

4. If a point of the BPP, $x$, is located at the origin, the remaining $N - 1$ points are uniformly distributed in $b_d(o, R)$. Thus, the pdf of the Euclidean distance from $x$ to its neighbors is identical to (2.4), with $N$ replaced by $N - 1$. Also note that (2.4) also holds for any reference point $x$ for which $0 \le r \le R - \|x\|$.

We wish to compare the distance distributions from the origin for an isotropic BPP and a PPP with the same density. However, in general, the PPP may have fewer points than the number dropped. In order to make a fair comparison, we condition on the fact that there are at least $N$ points present in the PPP model. The following corollary establishes the distance pdfs for such a conditioned PPP. Also note that conditioned on there being exactly $N$ points present, the PPP is equivalent to a BPP [9].

**Corollary 2.2.3.** *Consider a PPP of density $\lambda$ over a finite volume $b_d(o, R)$. Conditioned on there being at least $N$ points in the ball, the distance distribution from the origin to the $n^{th}$ nearest node ($n \le N$) is given by*

$$f'_{R_n}(r) = \frac{\lambda d c_d r^{d-1}\left(A_{n-1}(r)\left(\sum_{k=N-n}^{\infty} B_k(r)\right)\right)}{\sum_{k=N}^{\infty} A_k(R)}, \quad r \in [0, R], \tag{2.8}$$

*where $A_k(r) := e^{-\lambda c_d r^d}\left(\lambda c_d r^d\right)^k / k!$ and $B_k(r) := e^{-\lambda c_d \left(R^d - r^d\right)}\left(\lambda c_d \left(R^d - r^d\right)\right)^k / k!$.*

9

*Proof:* The complementary conditional cdf of $R_n$ is given by

$$
\begin{aligned}
\bar{F}'_{R_n}(r) &= \Pr\left(\Phi\left(b_d(o,r)\right) < n \mid \Phi\left(b_d(o,R)\right) \geq N\right) \\
&= \frac{\Pr\left(\Phi\left(b_d(o,r)\right) < n, \Phi\left(b_d(o,R)\right) \geq N\right)}{\Pr\left(\Phi\left(b_d(o,R)\right) \geq N\right)} \\
&\overset{(a)}{=} \frac{\sum_{k=0}^{n-1}\Pr\left(\Phi\left(b_d(o,r)\right) = k\right)\Pr\left(\Phi\left(b_d(o,R)\setminus b_d(o,r)\right) \geq N - k\right)}{\Pr\left(\Phi\left(b_d(o,R)\right) \geq N\right)} \\
&= \frac{\sum_{k=0}^{n-1} A_k(r)\left(1 - \sum_{l=0}^{N-k-1} B_l(r)\right)}{\sum_{k=N}^{\infty} A_k(R)},
\end{aligned}
\tag{2.9}
$$

where $(a)$ is obtained from the property that the number of points of the PPP in disjoint sets are independent of each other. It is easy to see that

$$
\frac{\mathrm{d}}{\mathrm{d}r} A_k(r) =
\begin{cases}
\lambda d c_d r^{d-1}\left(A_{k-1}(r) - A_k(r)\right) & k > 0 \\
-\lambda d c_d r^{d-1} A_0(r) & k = 0
\end{cases}
\tag{i}
$$

and

$$
\frac{\mathrm{d}}{\mathrm{d}r} B_l(r) =
\begin{cases}
\lambda d c_d r^{d-1}\left(B_l(r) - B_{l-1}(r)\right) & l > 0 \\
\lambda d c_d r^{d-1} B_0(r) & l = 0.
\end{cases}
\tag{ii}
$$

Therefore, we have

$$
\frac{\mathrm{d}}{\mathrm{d}r} \sum_{l=0}^{N-k-1} B_l(r) = \lambda d c_d r^{d-1} B_{N-k-1}(r).
\tag{iii}
$$

The details of the remainder of the proof are straightforward but tedious and are omitted here. Since the pdf of the conditional distance distribution is $f'_{R_n} = -\mathrm{d}\bar{F}'_{R_n}/\mathrm{d}r$, one basically has to differentiate the numerator in (2.9), and after some simplifications using (i)-(iii), it will be seen that the conditional distance pdf is identical to (2.8). $\qquad\square$

Fig. 2.2 depicts the pdfs of the distances for one- and two-dimensional BPPs (from (2.4)) and compares it with the distance pdfs for a conditioned PPP with the same density.

When a large number of points are distributed randomly over a large area, their arrangement can be well approximated by an infinite homogeneous PPP. The PPP model for the nodal distribution is ubiquitously used for wireless networks and may be justified by claiming that nodes are dropped from an aircraft in large numbers; for mobile ad hoc networks, it may be argued that terminals move independently of each other. We now present a corollary to the earlier theorem that reproduces a result from [12].
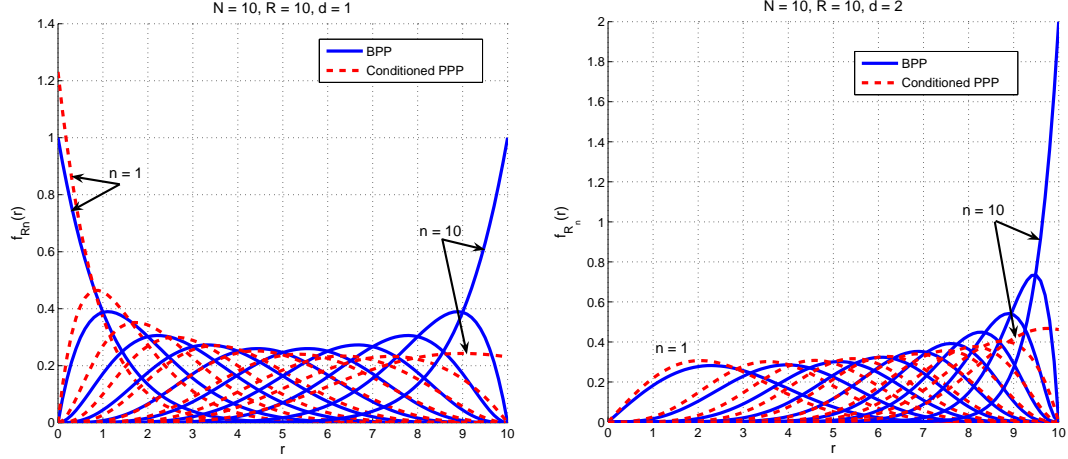
Figure 2.2. Distance pdfs for each of the neighbors for one- and two- dimensional binomial and conditioned Poisson networks with $N = 10$ and $R = 10$.

**Corollary 2.2.4.** *In an infinite PPP with density $\lambda$ on $\mathbb{R}^d$, the distance $R_n$, between a point and its $n^{th}$ neighbor is distributed according to the generalized gamma distribution.*

$$f_{R_n}(r) = e^{-\lambda c_d r^d} \frac{d(\lambda c_d r^d)^n}{r\Gamma(n)}, \quad r \in \mathbb{R}. \tag{2.10}$$

*Proof:* If the total number of points $N$ tends to infinity in such a way that the density $\lambda = N/(c_d R^d)$ remains constant, then the BPP asymptotically (as $R \to \infty$) behaves as a PPP [9]. Taking $R = \sqrt[d]{N/c_d\lambda}$ and applying the limit as $N \to \infty$, we obtain for a PPP,

$$
\begin{aligned}
f_{R_n}(r) &= \lim_{N\to\infty} \frac{d}{R} \frac{(1-p)^{N-n} p^{n-1/d}\Gamma(N+1)}{\Gamma(N-n+1)\Gamma(n)} \\
&= \frac{d}{r\Gamma(n)}(\lambda c_d r^d)^n \lim_{N\to\infty}\left(1 - \frac{\lambda c_d r^d}{N}\right)^N \frac{N(N-1)\ldots(N-n+1)}{N^n} \\
&= e^{-\lambda c_d r^d} \frac{d(\lambda c_d r^d)^n}{r\Gamma(n)}.
\end{aligned}
$$

for $r \in \mathbb{R}$. This is an alternate proof to the one provided in [12]. $\qquad\square$

11

## 2.3 Moments of the Internode Distances

We now consider the isotropic $d$-dimensional BPP and use the internode distance pdf (2.4) to compute its moments. The $\gamma^{\text{th}}$ moment of $R_n$ is calculated as follows[4].

$$
\begin{aligned}
\mathbb{E}[R_n^\gamma] &= \frac{d}{R}\frac{1}{B(N-n+1,n)}\int_0^R\left[r^\gamma\left(\frac{r}{R}\right)^{nd-1}\left(1-\left(\frac{r}{R}\right)^d\right)^{N-n}\right]\mathrm{d}r. \\
&\stackrel{(a)}{=} \frac{R^\gamma}{B(N-n+1,n)}\int_0^1 t^{n+\gamma/d-1}(1-t)^{N-n}\mathrm{d}t \\
&= \frac{R^\gamma}{B(N-n+1,n)}B_x(n+\gamma/d,N-n+1)|_0^1 \\
&\stackrel{(b)}{=} \begin{cases} \frac{R^\gamma\Gamma(N+1)\Gamma(\gamma/d+n)}{\Gamma(n)\Gamma(\gamma/d+N+1)} & \text{if } n+\gamma/d>0 \\ \infty & \text{otherwise} \end{cases} \\
&= \begin{cases} R^\gamma n^{[\gamma/d]}/(N+1)^{[\gamma/d]} & \text{if } n+\gamma/d>0 \\ \infty & \text{otherwise,} \end{cases}
\end{aligned}
\tag{2.11}
$$

where $B_x[a,b]$ is the incomplete beta function[5] and $x^{[n]}=\Gamma(x+n)/\Gamma(x)$ denotes the rising Pochhammer symbol notation. Here, $(a)$ is obtained by making the substitution $r=Rt^{1/d}$ and $(b)$ using the following identities:

$$
B_0(a,b) = \begin{cases} 0 & \mathcal{R}e(a)>0 \\ -\infty & \mathcal{R}e(a)\leq 0, \end{cases}
$$

and $B_1(a,b)=B(a,b)$ if $\mathcal{R}e(b)>0$.

The expected distance to the $n^{\text{th}}$ nearest node is thus

$$
\mathbb{E}(R_n) = \frac{Rn^{[1/d]}}{(N+1)^{[1/d]}},
\tag{2.12}
$$

and the variance of $R_n$ is easily calculated as

$$
\text{Var}[R_n] = \frac{R^2 n^{[2/d]}}{(N+1)^{[2/d]}} - \left(\frac{Rn^{[1/d]}}{(N+1)^{[1/d]}}\right)^2.
\tag{2.13}
$$

Remarks:

1. For one-dimensional networks, $\mathbb{E}[R_n]=Rn/(N+1)$. Thus, on an average, it is as if the points are arranged on a regular lattice. In particular, when $N$ is odd, the middle point is located exactly at the center on average.

---

[4]Note that $\gamma \in \mathbb{R}$ in general, and is not restricted to being an integer.
[5]Mathematica: Beta[x, a, b].

2. On the other hand, as $d \to \infty$, $\mathbb{E}[R_n] \to R$ and it is as if all the points are equidistant at maximum distance $R$ from the origin.

3. In the general case, the mean distance to the $n^{\text{th}}$ nearest node varies as $n^{1/d}$ for large $n$. This follows from the series expansion of the Pochhammer sequence[6] [17]

$$n^{[q]} = n^q \left(1 - O\left(1/n\right)\right).$$

   Also, for $d > 2$, the variance goes to $0$ as $n$ increases. This is also observed in the case of a Poisson network [12].

4. By the triangle inequality, the mean internodal distance between the $i^{\text{th}}$ and $j^{\text{th}}$ nearest nodes from the origin, $D_{ij}$, is bounded as (assuming $i < j$)

$$\frac{R\left(j^{[1/d]} - i^{[1/d]}\right)}{(N+1)^{[1/d]}} < \mathbb{E}[D_{ij}] < \frac{R\left(i^{[1/d]} + j^{[1/d]}\right)}{(N+1)^{[1/d]}}.$$

5. For the special case of $\gamma/d \in \mathbb{Z}$, we obtain

$$\mathbb{E}[R_n^\gamma] = R^\gamma \binom{n + \gamma/d - 1}{\gamma/d} \bigg/ \binom{N + \gamma/d}{\gamma/d}.$$

2.4   Distance Distributions in Regular Polygonal BPPs

In this section, we derive the pdf of the distance to the $n^{\text{th}}$ nearest node from the origin, in BPPs distributed on a $l$-sided regular polygon $W$. Assume that the polygon is centered at the origin and $|W| = A$. Then, its inradius and circumradius are respectively given by

$$R_{\text{i}} = \sqrt{\frac{A}{l} \cot\left(\frac{\pi}{l}\right)} \quad \text{and} \quad R_{\text{c}} = \sqrt{\frac{2A}{l} \csc\left(\frac{2\pi}{l}\right)}.$$

Also, let the total number of nodes be $N$ and assume that no point of the process is at the origin.

Clearly, when $r \le R_{\text{i}}$, $b_2(o, r)$ lies completely within the polygon and the number of points lying in it, $\Phi(b_2(o, r))$, is binomial distributed with parameters $n = N$ and $p = \pi r^2/A$.

When $R_{\text{i}} < r \le R_{\text{c}}$, $|W \cap b_2(o, r)|$ can be evaluated by considering the regions of the circle lying outside the polygon (see the shaded segment in Fig. 2.3). It is easy to see

---

[6]The notation $f(n) = O(g(n))$ means that there exists a constant $c$ and integer $N$ such that $f(n) \le cg(n)$ for $n > N$.
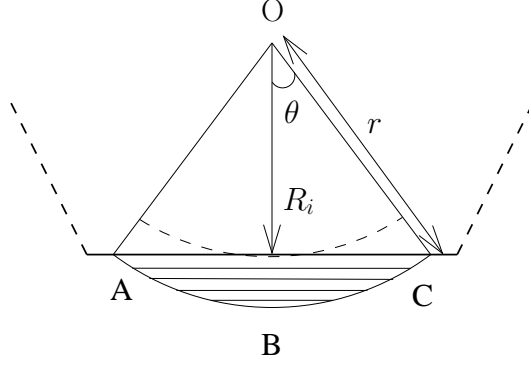
Figure 2.3. Section of a $l$-sided regular polygon depicting one of its sides. O is the origin. For $R_{\mathrm{i}} < r \le R_{\mathrm{c}}$, the area of the shaded segment ABC is $r^2\theta - R_{\mathrm{i}}\sqrt{r^2 - R_{\mathrm{i}}^2}$.

that $\Phi(b_2(o, r))$ follows a binomial distribution with parameters $n = N$ and

$$q = \frac{\pi r^2 - lr^2\theta + lR_{\mathrm{i}}\sqrt{r^2 - R_{\mathrm{i}}^2}}{A},$$

where $\theta = \cos^{-1}(R_{\mathrm{i}}/r)$. Following (2.3), we can write

$$f_{R_n}(r) = \begin{cases} \frac{2r\pi}{A}\frac{(1-p)^{N-n}p^{n-1}}{B(N-n+1,n)} & 0 < r \le R_{\mathrm{i}} \\ \frac{2r(\pi-l\theta)}{A}\frac{(1-q)^{N-n}q^{n-1}}{B(N-n+1,n)} & R_{\mathrm{i}} < r \le R_{\mathrm{c}} \\ 0 & R_{\mathrm{c}} < r. \end{cases} \tag{2.14}$$

Fig. 2.4 plots the pdf of the farthest neighbors in a BPP with 10 nodes, distributed on a $l$-sided regular polygon with $A = 100$, for $l = 3, 4, 5$ and $l \to \infty$.

## 2.5 Applications to Wireless Networks

We now apply the results obtained in the previous section to wireless networks. For the system model, we assume a $d$-dimensional network over a ball $b_d(o, R)$, where $N$ nodes are uniformly randomly distributed. Nodes are assumed to communicate with a base station (BS) positioned at the origin $o$. The attenuation in the channel is modeled by the large scale path loss function $g$ with PLE $\alpha$, i.e., $g(x) = \|x\|^{-\alpha}$. The channel access scheme is taken to be slotted ALOHA with contention parameter $\delta$.

### 2.5.1 Energy Consumption

The energy that is required to successfully deliver a packet over a distance $r$ in a medium with PLE $\alpha$ is proportional to $r^\alpha$. Therefore, the average energy required to
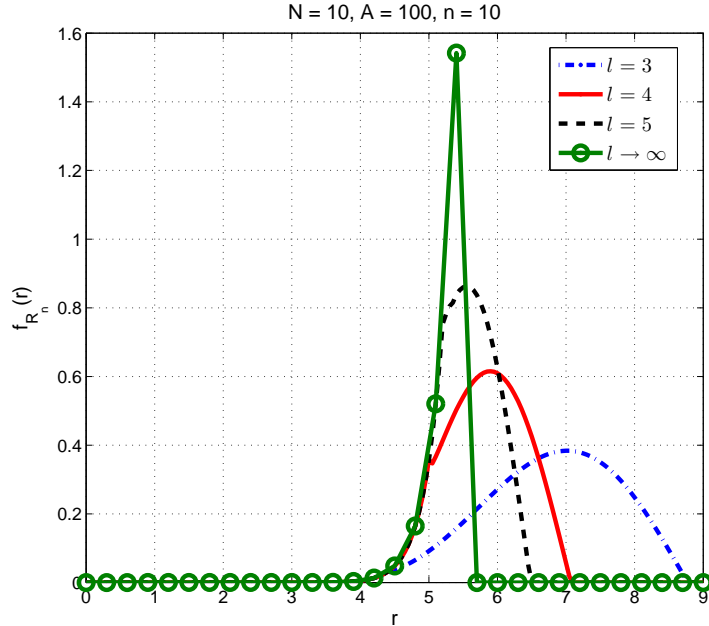
Figure 2.4. The pdf of the distances to the farthest nodes from the origin in a BPP with 10 nodes and area 100 units, distributed on a $l$-sided polygon for $l = 3, 4$ and 5. The dotted line depicts the farthest neighbor distance in a circle ($l \rightarrow \infty$), for which $R_i = R_c = 10/\sqrt{\pi}$.

deliver a packet from the $n^{\text{th}}$ nearest neighbor to the BS is given by (2.11), with $\gamma = \alpha$. This approximately scales as $n^{\alpha/d}$ when the routing is taken over single hops. When $\alpha < d$, it is more energy-efficient to use longer hops than when the PLE is greater than the number of dimensions.

### 2.5.2  Design of Routing Algorithms

The knowledge of nodal distances is also useful for the analysis and design of routing schemes for wireless networks. We illustrate this via an example wherein a greedy forwarding strategy that maximizes the expected progress of a packet towards its destination needs to be designed.

Consider the scenario where $N$ nodes are uniformly distributed in a disk of radius $R$. Assume that several packets need to be forwarded from the BS to an arbitrarily chosen destination node D, which lies far away from the BS. We also assume that each node has a peak (transmit) power constraint of $P \ll R^{\alpha}$. Let us suppose that the nodes adopt a

greedy forwarding strategy wherein each relay node $X_i$ that gets a packet relays it to its farthest neighbor in a sector of angle $\phi$ ($0 \leq \phi \leq \pi$), i.e., along $\pm \phi/2$ around the $X_i$-D axis (see Fig. 2.5). Evidently, for large $\phi$, the direction of the farthest neighbor in the sector may be off the $X_i$-D axis, while for small $\phi$, there may not be enough nodes inside the sector. The natural question to ask is: what value of $\phi$ maximizes the expected progress of packets[7] towards the destination?
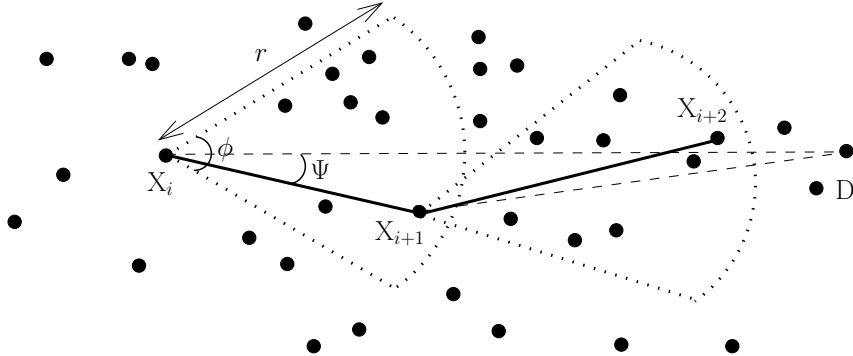


Figure 2.5. The greedy forwarding strategy. Each relay $X_i$ forwards the packet to its farthest neighbor lying inside the sector of radius $\phi$ around the $X_i$-D axis. The thick lines represent the path taken by the packet (through three arbitrary relays) for this particular realization.

A problem of similar flavor is studied in [18] for an interference-limited PPP, wherein the authors evaluate the optimal density of transmitters that maximizes the expected progress of a packet. In [19], the author determines the energy required to deliver a packet over a certain distance for various routing strategies in a PPP. In [20], the optimal transmission radius that maximizes the expected progress of a packet is determined for different transmission protocols in Poisson packet radio networks.

In order to evaluate the progress of a packet in the binomial network, we first note that if there are exactly $k$ nodes in an arbitrary sector of angle $\phi$ and radius $r = P^{1/\alpha}$ (which is the range of transmission), the average distance to the farthest ($k$th) neighbor in that sector is the same as $(2.12)$[8], with $n = k$, $R = r$ and $d = 2$. We also know that the number of nodes lying in that sector is binomial with parameters $N$ and $\left(r^2 \phi/2\pi R^2\right)$. Thus, the mean distance to the farthest neighbor in the considered sector can be written

---

[7]We define the progress of a packet from a relay node $X_i$ as the effective distance travelled along the $X_i$-D axis.

[8]This follows from the observation that in (2.1), the distance distributions depend only on $p = |b_2(x, r) \cap W|/|W|$, and the values of $p$ for the sector and the circle are the same.

as

$$\sum_{k=1}^{N} \binom{N}{k} \left(\frac{r^2\phi}{2\pi R^2}\right)^k \left(1 - \frac{r^2\phi}{2\pi R^2}\right)^{N-k} \frac{2rk}{2k+1}. \tag{2.15}$$

Note that the sectors emanating from nodes $X_i$ and $X_{i+1}$ overlap partially, and also, the total number of nodes is fixed; therefore the mean distance to the farthest neighbor, $\mathbb{E}[X']$, is actually upper-bounded by (2.15). However, since we consider the farthest neighbors, the sectoral overlap is small.

Next, let $\Psi$ denote the angle between the line connecting $X_i$ to its farthest neighbor ($X_{i+1}$) and the $X_i$-D axis. Since the nodal distribution is uniformly random, $\Psi$ is uniformly distributed on $[-\phi/2, \phi/2]$. The expected progress of a packet is $\mathbb{E}[X] = \mathbb{E}[X']\mathbb{E}[\cos(\Psi)]$ since $\Psi$ and $X'$ are independent of each other, and is upper-bounded as

$$\mathbb{E}[X] \le \frac{2}{\phi} \sin\left(\frac{\phi}{2}\right) \sum_{k=1}^{N} \frac{2P^{1/\alpha}k}{2k+1} \binom{N}{k} \left(\frac{P^{2/\alpha}\phi}{2\pi R^2}\right)^k \left(1 - \frac{P^{2/\alpha}\phi}{2\pi R^2}\right)^{N-k}. \tag{2.16}$$

The optimum value of $\phi$ that maximizes the progress of packets can be numerically determined from (2.16).

Fig. 2.6 plots the expected progress of a packet (upper bound) versus $\phi$ for several values of $N$ using (2.16), and compares it with the empirical value, obtained via simulation. We see that the bound is reasonably tight, in particular at lower $N$. The optimum values of $\phi$ are also marked in the figure.

### 2.5.3   Localization

In wireless networks, localization is an integral component of network self-configuration. Nodes that are able to accurately estimate their positions can support a rich set of geographically aware protocols and report the regions of detected events. Localization is also useful for performing energy-efficient routing in a decentralized fashion.

In this section, we investigate conditional distance distributions and study their usefulness to localization algorithms. We consider the scenario wherein a few nodes precisely know or can accurately estimate their distances from the BS. What can be said about the distance statistics of the other nodes given this information?

Suppose we know that the $k^{\text{th}}$ nearest neighbor is at distance $s$ from the center[9]. Then, clearly, the first $k-1$ nodes are uniformly randomly distributed in $b_d(o, s)$ while the

---

[9]Based on the RSS from the base station, perhaps averaged over a period of time to eliminate the variations due to fading, nodes can determine how many other nodes are closer to the transmitter than they are. This way, a node would find out that it is the $k^{\text{th}}$ nearest neighbor to the base station.
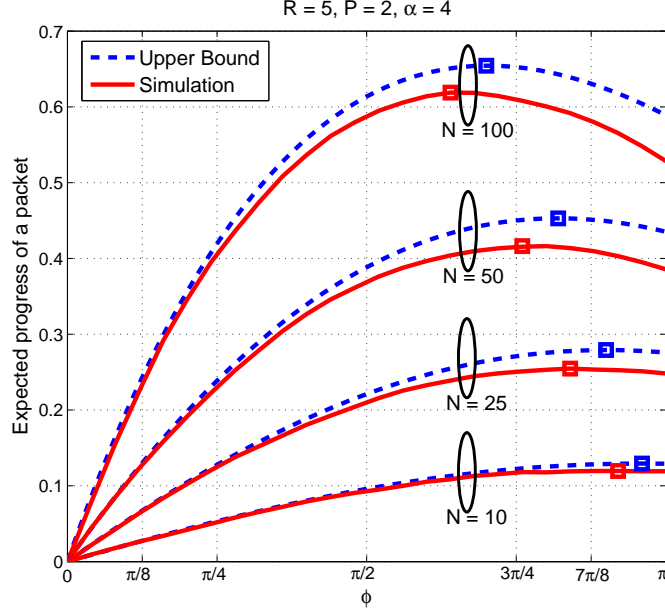
Figure 2.6. The expected progress of a packet (empirical and upper bound) for various values of $N$. The square markers correspond to the optimum values of $\phi$ that maximize the packet's progress.

more distant nodes are uniformly randomly distributed in $b_d(o, R) \setminus b_d(o, s)$. Following (2.4), the distance distributions of the first $k - 1$ nearest neighbors from the origin can be written as

$$f_{R_n}(r \mid R_k = s) = \frac{d}{s} \frac{B(n - 1/d + 1, k - n)}{B(k - n, n)} \beta \left( \left( \frac{r}{s} \right)^d ; n - \frac{1}{d} + 1, k - n \right), \quad n < k$$

for $0 \leq r \leq s$, which again follows a generalized beta distribution.

For the remaining nodes, i.e., for $n > k$, we have in $r \in [s, R]$,

$$\begin{aligned} f_{R_n}(r \mid R_k = s) &= -\frac{\mathrm{d}}{\mathrm{d}r} I_{1-q}(N - n + 1, n - k) \\ &= \frac{dr^{d-1}}{R^d - s^d} \frac{(1 - q)^{N-n} q^{n-k-1}}{B(N - n + 1, n - k)} \end{aligned}$$

where $q = (r^d - s^d)/(R^d - s^d)$.

The moments of $R_n$ are also straightforward to obtain. Following (2.11), we see that for $n < k$ and $n + \alpha/d > 0$,

$$\mathbb{E}[R_n^\alpha \mid R_k = s] = \frac{s^\alpha n^{[\alpha/d]}}{(k + 1)^{[\alpha/d]}}. \tag{2.17}$$

For $n > k$, we have

$$
\begin{aligned}
\mathbb{E}[R_n^\alpha \mid R_k = s] &= \int_s^R \frac{dr^{\alpha+d-1}}{R^d - s^d} \frac{(1-q)^{N-n} q^{n-k-1}}{B(N-n+1, n-k)} dr \\
&= \frac{1}{B(N-n+1, n-k)} \int_0^1 q^{n-k-1}(1-q)^{N-n} \left(q\left(R^d - s^d\right) + s^d\right)^{\alpha/d} dq \\
&= \frac{s^\alpha}{(n-k)B(N-n+1, n-k)} F_1\left(n-k; n-N, -\frac{\alpha}{d}; n-k+1; 1, 1 - \frac{R^d}{s^d}\right),
\end{aligned}
$$

where $F_1[a; b_1, b_2; c; x, y]$ is the Appell hypergeometric function of two variables[10].

Often, it is easiest to measure the nearest-neighbor distance. Give this distance as $s$, we have for $n > 1$,

$$
f_{R_n}(r \mid R_1 = s) = \frac{dr^{d-1}}{R^d - s^d} \frac{\left(1 - \left(\frac{r^d - s^d}{R^d - s^d}\right)\right)^{N-n} \left(\frac{r^d - s^d}{R^d - s^d}\right)^{n-2}}{B(N-n+1, n-1)}
$$

for $r \in [s, R]$. Also, the mean conditional distances to the remaining neighbors are

$$
\mathbb{E}[R_n \mid R_1 = s] = \frac{s}{(n-1)B(N-n+1, n-1)} F_1\left(n-1; n-N, -\frac{1}{d}; n-1; 1, 1 - \frac{R^d}{s^d}\right).
$$

Fig. 2.7 plots the mean conditional distances in a network with 10 nodes when the nearest-neighbor distance is unity.

### 2.5.4 Interference

In order to accurately determine network parameters such as outage, throughput or transmission capacity, the interference in the system $I$ needs to be known.

Let $T_n \in \{0, 1\}$, $1 \leq n \leq N$ denote the random variable representing whether the $n^{\text{th}}$ nearest node to the BS transmits or not, in a particular time slot. With the channel access scheme being ALOHA, these are i.i.d. Bernoulli variables (with parameter $\delta$).

The mean interference as seen at the center of the network is given by

$$
\begin{aligned}
\mu_I &= \mathbb{E}\left[\sum_{n=1}^N (T_n R_n^{-\alpha})\right] = \sum_{n=1}^N \mathbb{E}[T_n]\mathbb{E}\left[R_n^{-\alpha}\right], \\
&= \delta \sum_{n=1}^N \mathbb{E}\left[R_n^{-\alpha}\right].
\end{aligned}
$$

Setting $\gamma = -\alpha$ and $n = 1$ in (2.11), we can conclude that the mean interference is infinite for $d \leq \alpha$. This is due to the nearest interferer. Even the mean interference from (just) the $n^{\text{th}}$ nearest transmitter is infinite if $\alpha \geq nd$. When the number of dimensions

---

[10]Mathematica: AppellF1[a, b1, b2, c, x, y].
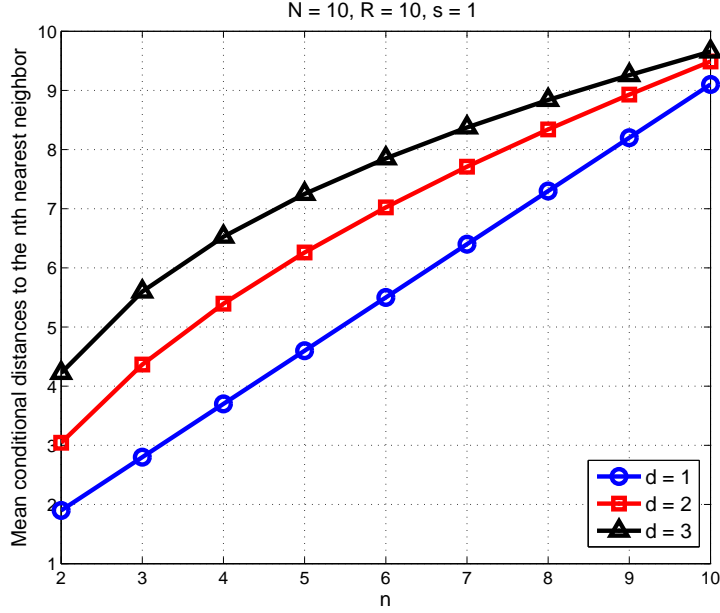
Figure 2.7. The mean conditional distances of the higher-order neighbors in a binomial network with 10 nodes and $d = 1, 2, 3$, when it is known that the nearest neighbor is at unit distance away from the base station.

is greater than the PLE, we have

$$\mu_I = \frac{\delta R^{-\alpha} \Gamma(N+1)}{\Gamma(N+1-\alpha/d)} \sum_{n=1}^{N} \frac{\Gamma(n-\alpha/d)}{\Gamma(n)}.$$

One can inductively verify that

$$\sum_{n=1}^{k} \frac{\Gamma(n-\alpha/d)}{\Gamma(n)} = \frac{\Gamma(k-\alpha/d)}{\Gamma(k)} \frac{k-\alpha/d}{1-\alpha/d} \quad \forall k \in \mathbb{Z}, \tag{2.18}$$

and we obtain after some simplifications,

$$\mu_I = \frac{N\delta d R^{-\alpha}}{d-\alpha}, \quad d > \alpha. \tag{2.19}$$

The unboundedness of the mean interference at practical values of $d$ and $\alpha$ (i.e., $d < \alpha$) actually occurs due to the fact that the path loss model we employ breaks down for very small distances, i.e., it exhibits a singularity at $x = 0$. One way to overcome this issue is to impose a guard zone of radius $\epsilon$ around every receiver. In other words, every receiver has an exclusion zone of radius $\epsilon$ around it and the nodes lying within it are not allowed to transmit.

Since the average number of nodes in the ball $b(o, \epsilon)$ is $N\epsilon^d/R^d$, we obtain the mean interference in this case to be

$$
\begin{aligned}
\mu_I &= \frac{NpdR^{-\alpha}}{d - \alpha} - \frac{N\epsilon^d \delta d\epsilon^{-\alpha}}{R^d(d - \alpha)} \\
&= \frac{N\delta d(R^{d-\alpha} - \epsilon^{d-\alpha})}{R^d(d - \alpha)}, \quad \forall d \neq \alpha.
\end{aligned}
\tag{2.20}
$$

Taking limits, we obtain $\mu_I = N\delta d \ln(R/\epsilon)/R^d$ when $d = \alpha$.

Alternatively, authors have used different path loss model laws such as $\min\{1, \|x\|^{-\alpha}\}$, $1 + \|x\|^{-\alpha}$ or $\exp(-\|x\|)$ to keep the interference term bounded in their analyses.

### 2.5.5 Outage Probability and Connectivity

Assuming that the system is interference-limited, an outage $\mathcal{O}$ is defined to occur if the SIR at the BS is lower than a certain threshold $\Theta$. Let the desired transmitter be located at unit distance from the origin, transmit at unit power and also not be a part of the original point process. Then, the outage probability is $\Pr(\mathcal{O}) = \Pr[1/I < \Theta]$. Considering only the interference contribution from the nearest neighbor to the origin, a simple lower bound is established on the outage probability as

$$
\begin{aligned}
\Pr(\mathcal{O}) &\geq \Pr\left(T_1 R_1^{-\alpha} > 1/\Theta\right) \\
&= \delta \Pr\left(R_1 < \Theta^{1/\alpha}\right) \\
&= \begin{cases} \delta\left(1 - \left(1 - \frac{\Theta^{d/\alpha}}{R^d}\right)^N\right) & \Theta \leq R^\alpha \\ \delta & \Theta > R^\alpha. \end{cases}
\end{aligned}
\tag{2.21}
$$

The empirical values of success probabilities and their upper bounds (2.21) are plotted for different values of $N$ in Fig. 2.8. As the plot depicts, the bounds are tight for lower values of $N$ and $\Theta$, and therefore we conclude that the nearest neighbor contributes most of the network interference. However, as $\alpha$ decreases, the bound gets looser since the contributions from the farther neighbors are (also) increased.

Next we study the connectivity properties of the binomial network, assuming that interference can be controlled such that the system is noise-limited. Define a node to be connected to the origin if the SNR at the BS is greater than a threshold $\Theta$. Let the nodes transmit at unit power and assume noise to be AWGN with variance $N_0$. In the absence of interference, the probability that the BS is connected to its $n^{\text{th}}$ nearest
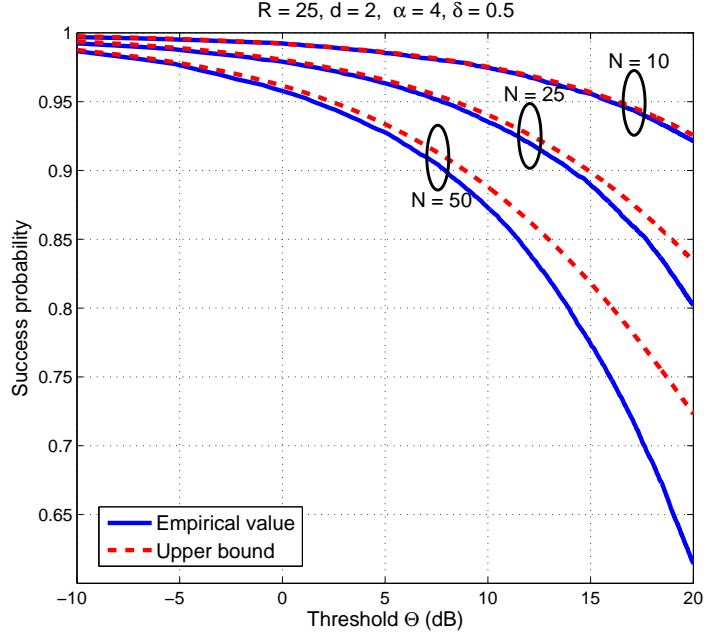
Figure 2.8. Comparison of exact success probabilities versus their upper bounds for different values of the system parameters.

neighbor is

$$\begin{aligned}
\Pr(R_n^{-\alpha} > N_0\Theta) &= 1 - \Pr(R_n > (N_0\Theta)^{-1/\alpha}) \\
&= \begin{cases} 1 - I_{1-p'}(N - n + 1, n) & \Theta > R^{-\alpha}/N_0 \\ 1 & \Theta \leq R^{-\alpha}/N_0, \end{cases}
\end{aligned} \quad (2.22)$$

where $p' = \left((N_0\Theta)^{-1/\alpha}/R\right)^d$. Fig. 2.9 plots the connection probability in a two-dimensional binomial network with 25 nodes.

The mean number of nodes that are connected to the BS is $N \min\{1, \left(\frac{(N_0\Theta)^{-1/\alpha}}{R}\right)^d\}$.

### 2.5.6 Other Applications

We now list a few other areas where knowledge of the distance distributions is useful.

- *Routing*: The question of whether to route over smaller or longer hops is an important, yet a nontrivial issue [21, 22], and it gets more complicated in the presence of interference in the network. The knowledge of internodal distances is necessary for evaluating the optimum hop distance and maximizing the progress of a packet towards its destination.
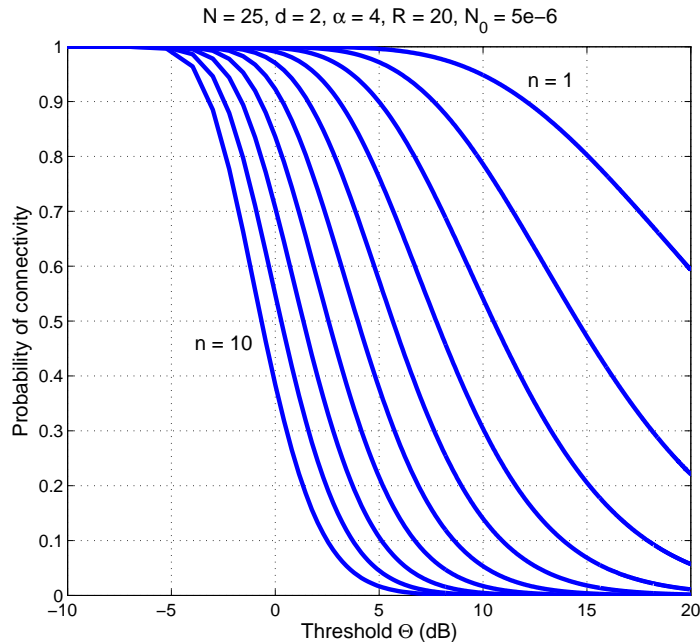
Figure 2.9. The probability of the $n^{\text{th}}$ nearest neighbor, $n = 1, 2, \ldots, 10$, being connected to the BS (2.22) for a binomial network with 25 nodes.

- *Path loss exponent estimation*: The issue of PLE estimation is a very important and relevant problem [23]. Several PLE estimation algorithms are based on received signal strength techniques, which require the knowledge of distances between nodes.

2.6  Chapter Summary

We argue that the Poisson model for nodal distributions in wireless networks is not accurate in many practical situations and instead consider the often more realistic binomial network model. We derive exact analytical expressions for the pdfs of the internodal distances in a network where a known number of nodes are independently distributed in a compact set. Specializing to the case of an isotropic random network, we show that the distances between nodes follow a generalized beta distribution and express the moments of these random variables in closed-form. We also derive the distribution of the internodal distances for the BPP distributed on a regular polygon. Our findings have applications in several problems relating to wireless networks such as energy consump-

tion, design of efficient routing and localization algorithms, connectivity, interference characterization and outage evaluation. We conclude that distance distributions are a useful tool in analyzing single-hop characteristics of ad hoc networks.

CHAPTER 3

TASEPS: A STATISTICAL MECHANICS TOOL TO ANALYZE THE
PERFORMANCE OF WIRELESS LINE NETWORKS

3.1  Introduction

A wireless ad hoc network is typically formed by deploying nodes that possess self-
organizing capabilities. Due to the stringent energy constraint in these devices, a natural
communication strategy to conserve battery life is to reduce the range of transmission
and employ multihop routing, where relays assist in the delivery of packets from the
source to the destination. Multihop wireless networks are not just intended to carry
small volumes of data in an energy-efficient manner, but may also be used to provide
broadband services, for example in mesh networks. However, existing buffering schemes
for multihop wireless networks involving large buffer sizes and a drop-tail policy have cer-
tain inherent drawbacks such as buffer overflows, excessive queueing delays and schedul-
ing issues resulting in uncoordinated transmissions. Consequently, the end-to-end delay
and throughput performance in such systems is disappointing [24]-[26].

The contribution of this chapter is two-fold:
First, we propose a simple buffering and channel access scheme to overcome the afore-
mentioned shortcomings. Accordingly, the buffer sizes at relay nodes are restricted to
just one packet, and all the buffering is pushed back to the source node. Also, nodes
transmit packets only if their adjacent nodes' buffer is empty, and packets are retrans-
mitted until they are successfully received. We shall see that employing this modified
transmission policy not only keeps scheduling simple but also helps regulate the flow of
packets in a completely decentralized fashion. It maintains a certain spacing between
packets which is essential for the efficient operation of systems.
Second, we characterize the end-to-end delay and achievable throughput of the wire-
less multihop line network employing the revised buffering policy. While most prior

work has focused only on average delays and neglected characterizing the correlations between delays across different hops (or worked around this issue by assuming multiple traffic flows), we also explicitly derive the spatial delay correlations in the network. Additionally, we provide applications of our findings for large wireless line networks.

For our analysis, we consider two slotted channel access methods that are tractable: randomized TDMA (r-TDMA) and slotted ALOHA. r-TDMA is a modified version of the traditional TDMA, wherein the transmitting node in each time slot is chosen uniformly randomly from the set of all nodes instead of being picked in an ordered fashion. In the ALOHA-based network, in each time slot, each node having a packet independently transmits with a certain probability. To simplify the analysis, we exploit the analogy between multihop wireless line networks and the discrete-time *totally asymmetric simple exclusion process* (TASEP) [27], a stochastic process in statistical mechanics which has also been used to analyze other interesting problems such as the kinetics of biopolymerization and traffic. In particular, we focus on the TASEP models with random sequential and parallel updates. In addition, we describe other TASEP types, namely the sequential TASEP and the sub-lattice parallel TASEP which can be linked to the classical TDMA and spatial TDMA MAC schemes, respectively. This work is intended to enhance our understanding of the dynamics of packet transport in multihop wireless networks.

3.2   System Model

We consider a multihop wireless line network with a unidirectional data flow from the leftmost to the rightmost node. The source node S is numbered 0 and generates packets of fixed length at a constant rate. The network contains $N$ relay nodes (numbered 1 through $N$) and a destination D. Each node has a buffer of size $K \geq 1$ packets. The arrangement of nodes is regular (on a lattice) with a separation of $l$ between any pair of adjacent nodes. Time is slotted to the duration of a packet, and transmission attempts occur at slot boundaries.

In this chapter, we consider the case where all the nodes in the network use the same channel and assume that simultaneous transmissions cause interference between links. We take the attenuation in the channel to be modeled according to the large-scale path loss law with exponent $\gamma$. The noise in the network is taken to be AWGN

with variance $N_0$. We define the transmission from node $i$ to node $j$ to be successful if the (instantaneous) signal-to-interference-and-noise ratio (SINR) at $j$ is greater than a predetermined threshold $\Theta$. The probability of successful reception is denoted by $p_s = \Pr\left[\text{SINR} > \Theta\right]$.

### 3.3 Motivation

#### 3.3.1 Optimality of ALOHA: The Sufficiency of Small Buffers

Assume for now that at any receiver node, only the nearest interferer contributes to the interference. Let $m$ denote the *spatial-reuse parameter*, which is the minimum number of hops separating any two transmitters $i$ and $j$ such that both their transmissions are successful. Indeed, if each node transmits with power $P$, we require

$$p_s = 1 \quad \Leftrightarrow \quad \frac{Pl^{-\gamma}}{P(ml-l)^{-\gamma} + N_0} > \Theta. \tag{3.1}$$

It is straightforward to see that

$$m = \left\lceil \left( \frac{1}{\Theta} - \frac{N_0}{Pl^{-\gamma}} \right)^{-1/\gamma} \right\rceil + 1 \tag{3.2}$$

is the spatial-reuse parameter that satisfies (3.1).

For the system model considered, the optimal throughput at steady state is equal to $1/m$; it is achieved when each $m^{\text{th}}$ node transmits simultaneously. Also, in this case, the steady state end-to-end delay is minimal and equal to $N+1$ time slots. The optimal scheduling of the multihop wireless network that minimizes the end-to-end delay (and maximizes the throughput) is illustrated in Fig. 3.1, for certain values of the system parameters. Note that this MAC scheme is equivalent to a simple slotted ALOHA protocol (with transmit probability 1), in which every node that has a packet in its buffer transmits.

In the above scenario, all the transmissions are successful. However, in the presence of fading, unequal spacing between the nodes, or interference from other networks, transmissions can fail, and the slotted ALOHA scheme with contention parameter 1 may perform sub-optimally. Nevertheless, this example illustrates that for the efficient operation of networks, it is necessary that the transmitting nodes not be too closely located. In fact, for half-duplex nodes, $m$ needs to be always kept $\geq 2$. This example also illustrates that since adjacent nodes cannot both transmit successfully at the same time,
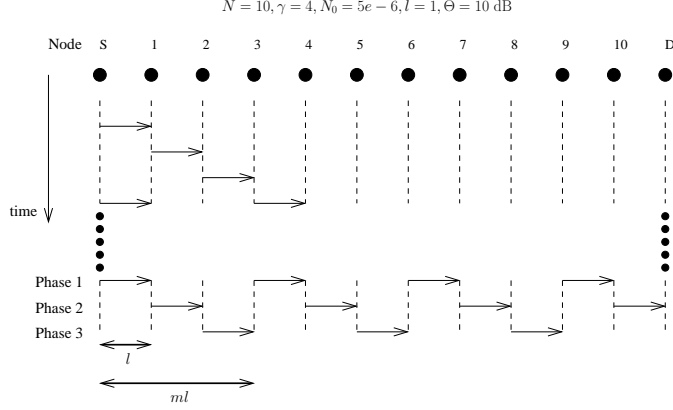
Figure 3.1. The optimal scheduling assignment (in the absence of fading) for a multihop line network with 10 relay nodes. For the system parameters specified, $m = 3$. In the steady state, there are three unique transmission phases, in each of which nodes three hops apart transmit simultaneously. The system achieves a throughput of 1/3 and an end-to-end delay of 11 time slots.

it is not necessary to have $K > 1$ as packets are never stacked; small buffers ($K = 1$) are sufficient for the optimal operation of the network.

### 3.3.2   A Revised Transmission Policy

Motivated by the straightforward yet optimal ALOHA protocol, we propose a simplified transmission policy for multihop wireless networks characterized by the following three rules.

1. All the buffering is performed at the source node, while relay nodes are essentially bufferless (have buffer sizes of unity).

2. Transmissions are not attempted by nodes if their adjacent node's buffer already contains a packet.

3. Packets are retransmitted until they are successfully received.

Rule 1 ensures that nodes have at most one packet in their buffer and is favorable for the following reasons.

- First, for $K = 1$, the scheduling scheme can be made very simple and completely decentralized: nodes that have a packet transmit and others remain idle. As in

28

the case of the throughput-achieving ALOHA scheme illustrated earlier, the interference in the network induces a natural spacing between packets, and all nodes with a packet can simultaneously transmit successfully with a high probability of success. When multiple packets are present at nodes however, the spacing between packets is not preserved and hence, more complicated (and perhaps, centralized) scheduling algorithms are needed.

- Second, keeping the value of $K$ small can prevent the average end-to-end delay from getting excessive without the source knowing about it. Indeed, for a general MAC scheme, several packets may get stacked-up in a buffer when $K$ is large, especially when the link quality is poor, and transportation of packets across links get delayed. Moreover, since packets are backlogged over multiple relays, the average end-to-end delay at steady state becomes huge.

  Due to stacking-up of packets at buffers, the variance of the end-to-end delay also increases with buffer size. In other words, in the single-buffer case, the delay incurred after the packet leaves the source is much more tightly controlled than in the multiple-buffer case. Depending on the time a packet spends at the first relay, the source node can make a more judicious decision on whether to drop a packet or not.

- Third, large buffers increase hardware cost and energy consumption.

However, using Rule 1 alone may lead to a loss in throughput due to dropped packets, and Rule 2 is needed mainly to reduce interference and consequently keep the number of failed transmissions small. In fact, Rules 1 and 2 together mean that a transmission can occur only when a node has a packet to transmit and its target node has an empty buffer. This is a simple, distributed way to prevent packets from getting too closely spaced and ensure that the transmitting nodes will be at least two hops apart. A simple way to enforce the latter rule is by having relay nodes ignore incoming request-to-send (RTS) or send a negative clear-to-send (CTS) if their buffers are full. Rule 3 ensures that the network is 100% reliable. Together, the rules help regulate the flow of packets in the network in a completely distributed fashion. The revised transmission scheme also intrinsically enforces congestion control and works similar to reactive back-pressure

algorithms (see for example, [28]) wherein the load at each server is balanced dynamically based on the states of upstream and downstream queues.

In this chapter, we characterize the delay and throughput performance of multihop wireless networks, employing the aforementioned transmission scheme, for two different MAC schemes, the r-TDMA and slotted ALOHA. For our analysis, we use some existing results from the TASEP literature.

## 3.4  Related Work

### 3.4.1  Review of Literature

The delay and throughput performances of the classical TDMA, spatial TDMA, ALOHA and several other MAC schemes have been extensively studied for point-to-point links using queueing-theoretic approaches [29]-[32]. However, there is limited work on the performance analysis of networks with multiple hops [33]-[35] since their analysis is less tractable and often yields only approximate results. In order to circumvent analytical issues, authors have considered very small [36]-[38] or infinitely large [39, 40] networks. Additionally, previous studies have either considered unlimited buffer capacities [41] or neglected queueing delays in the system [42], both of which are not realistic assumptions. In this work, we use existing results from the TASEP literature to derive exact analytical results on the throughput and delay performance of wireless line networks with an arbitrary number of nodes. Also, since we consider relays with unit buffers, the queueing delays at nodes are clearly zero, and we only need to consider access and retransmission delays.

The benefits of keeping relay buffer sizes equal to unity has been studied earlier in literature. In [43], the author considers a buffering policy similar to the one described earlier in this chapter, and proposes several amendments to the MAC layer, such as the notion of *shadow packets* to stabilize the system and achieve the optimal throughput. In [44], the authors show that buffering and network coding implemented at the source node can lead to comparable packet drop rates compared to buffering at every intermediate router. In the case of large networks with multiple links, the coding-based scheme can also provide buffer gains.

### 3.4.2 A Review of TASEPs with Open Boundaries

We now provide a short review of the discrete-time one-dimensional TASEP with open boundaries and furnish details on four commonly studied updating procedures, namely random sequential, ordered sequential, sublattice-parallel and parallel. We also briefly introduce the *matrix product ansatz* (MPA), an algebraic framework that is used extensively later in the chapter.

The TASEP refers to a family of simple stochastic processes used to describe the dynamics of self-driven systems with several interacting particles and is a paradigm for non-equilibrium systems [45, 46]. The classical 1D TASEP model with open boundaries is defined as follows. Consider a system with $N + 1$ sites, numbered 0 to $N$. Site 0 is taken to be the source that injects particles into the system. The model is said to have open boundaries, meaning that particles are injected into the system at the left boundary (site 1) and exit the system on the right boundary (site $N$). The occupancy of site $i$, $1 \leq i \leq N$ is denoted by $\tau_i$. At any given time, site $i$ can either be occupied ($\tau_i = 1$) or empty ($\tau_i = 0$). This form of an exclusion principle leads to interesting dynamical properties, as we shall see later. The source node is taken to be always occupied ($\tau_0 \equiv 1$).

In the discrete-time version of the TASEP, the movement of particles is defined to occur in time steps. Specifically, let $(\tau_1[t], \tau_2[t], \ldots, \tau_N[t]) \in \{0, 1\}^N$ denote the configuration of the system at time slot $t$. In the subsequent time slot $t + 1$, one chooses a single site or a set of sites depending on the updating procedure. For every site picked, if it contains a particle and the neighboring site on its right has none, then the particle hops from that site to its neighbor with a certain probability. This way, the particles are transported from site 0 through the system until their eventual exit at site $N$.

The dynamics of the classical TASEP particle flow is defined as follows. Suppose that the $i^{\text{th}}$ site is chosen in time slot $t$.

If $1 \leq i \leq N - 1$, the particle on site $i$ (if there is any) jumps to site $i + 1$ (provided it is empty) with probability $p$. Accordingly,

$$
\begin{aligned}
\mathbb{P}(\tau_i[t+1] = 0) &= 1 - \tau_i[t](1 - p + p\tau_{i+1}[t]) \\
\mathbb{P}(\tau_i[t+1] = 1) &= \tau_i[t](1 - p + p\tau_{i+1}[t]).
\end{aligned}
$$

and

$$\mathbb{P}(\tau_{i+1}[t+1] = 0) = (1 - \tau_{i+1}[t])(1 - p\tau_i[t])$$

$$\mathbb{P}(\tau_{i+1}[t+1] = 1) = p\tau_i[t] + \tau_{i+1}[t](1 - p\tau_i[t]).$$

If $i = 0$, site 1 remains occupied at time $t + 1$ if it was occupied at time $t$ and gets occupied with probability $\alpha$ if it was empty. Thus,

$$\mathbb{P}(\tau_1[t+1] = 0) = (1 - \alpha)(1 - \tau_1[t])$$

$$\mathbb{P}(\tau_1[t+1] = 1) = \alpha + (1 - \alpha)\tau_1[t].$$

If $i = N$, site $N$ remains empty at $t+1$ if it was empty at time $t$, and gets emptied with probability $\beta$ if it was occupied, i.e.,

$$\mathbb{P}(\tau_N[t+1] = 0) = 1 - (1 - \beta)\tau_N[t]$$

$$\mathbb{P}(\tau_N[t+1] = 1) = (1 - \beta)\tau_N[t].$$

A snapshot of the TASEP system model is depicted in Fig. 3.2. The particle that jumps leaves a *hole* behind. Therefore, hopping of particles to the right results in the holes moving to the left towards the source, hence the system exhibits a *particle-hole symmetry* and studying only the first $\lceil (N+1)/2 \rceil$ sites is sufficient to characterize the system completely.
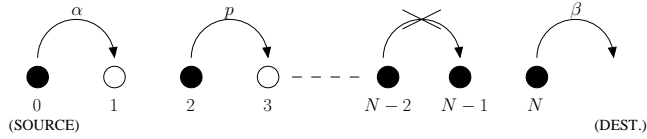


Figure 3.2. Snapshot of a TASEP system model along with the hopping probabilities. The source is numbered 0, and there are $N$ other sites. Filled circles indicate occupied sites and the rest indicate holes. Jumping from site $i$ is possible only if the configuration $\{\tau_i, \tau_{i+1}\}$ is $\{1,0\}$. In the above example, hopping is not possible between sites $N - 2$ and $N - 1$.

The TASEP model is known to exhibit rich non-equilibrium behavior, even at steady state, where the rate of particle flow between any two adjacent sites is a constant. Here, the non-equilibrium nature of the model refers to the fact that the source and destination nodes are never at equilibrium, i.e., data always flows from the source node to the destination node. In this dynamical system, it is of interest to compute the steady state

probabilities of the particle configurations, the occupancies of the sites and the rate of particle flow [45, 46]. The values of the aforementioned quantities, however, explicitly depend on the updating procedure, i.e., the order in which the spatio-temporal hopping, injection and removal of particles is performed. There are four basic and commonly considered TASEP updating procedures:

1. *Random-sequential update*: A site is randomly picked with a uniform probability of $1/(N+1)$ at each time step. Hopping is performed based on rules defined above with probabilities $\alpha$, $\beta$ and $p$ for particles at sites $i = 0$, $i = N$ and $i \notin \{0, N\}$ respectively.

2. *Sublattice-parallel update*: Assume that the number of sites $N$ is even. We first apply injection (removal) rules to sites $0$ ($N$) and also perform hopping on pairs $(2, 3)$, $(4, 5)$, and so on. In the subsequent time step, updating rules are applied to site pairs $(1, 2)$, $(3, 4)$, etc.

3. *Ordered-sequential update*: As the name suggests, this is a procedure where updating is performed in an orderly, sequential fashion. One usually starts from the right end of the chain and updates the particle at node $N$. Then, the pairs $(N - 1, N)$, $(N - 1, N - 2)$, and so on are updated until the left end of the chain (node 0) is reached. In this form of updating, a series of adjacent particles can all be transported sequentially, unlike the previous updating schemes.

4. *Parallel update*: The updating rules are simultaneously applied to all the sites, and in each time slot, all particles at sites that have an empty site to their right jump simultaneously. This updating scheme is often used to model vehicular traffic flow and is a special case of the well-known Nagel-Schreckenberg model [47].

It is apparent from the description of the TASEP model that it exhibits a similarity to wireless line networks. The sites can be taken to represent the relay nodes and the particles the packets. The exclusion principle models the unit buffer size at the relay nodes. All the buffering in the network has to occur at the source. We assume that the original source has a large buffer and regulates the flow of data into a TASEP source, by sending in packets to the network only when it is chosen for transmission. The resulting system model is depicted in Fig. 3.3.
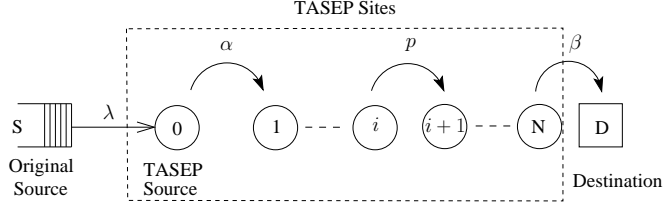
Figure 3.3. The system model. The wireless line network is modeled as a source node with a large buffer connected to the TASEP particle flow model with $N+1$ sites, each with a buffer size of unity.

### 3.4.3  Matrix Product Ansatz

The starting point in solving for the steady state solution of the one-dimensional TASEP model is to write down the *master equation*. Let $\mathbb{P}_N(\tau, t)$ denote the probability of finding the system in the configuration $\tau = (\tau_1, \tau_2, \ldots, \tau_N)$ in time slot $t$. The master equation describes the evolution of the system with time and takes the form

$$\Delta\left(\mathbb{P}_N(\tau, t)\right) = \sum_{\tau'}\left[\xi(\tau', \tau)\mathbb{P}_N(\tau', t) - \xi(\tau, \tau')\mathbb{P}_N(\tau, t)\right],$$

where $\Delta\left(\mathbb{P}_N(\tau, t)\right) = \mathbb{P}_N(\tau, t+1) - \mathbb{P}_N(\tau, t)$, and $\xi(\tau, \tau')$ denotes the rate of transition from $\tau$ to $\tau'$. We now associate to every configuration $\tau$ a column vector $|\tau\rangle$ (represented here by the "ket" notation) defining an orthonormal basis, with $\langle\tau'|\tau\rangle = \delta_{\tau', \tau}$, and define the state of the system at time $t$ as

$$|\mathbb{P}_N[t]\rangle = \sum_{\tau}\mathbb{P}_N(\tau, t)|\tau\rangle.$$

For the TASEP with random sequential update, one needs to only consider interactions between nearest neighbors, and it is possible write $\Delta|\mathbb{P}_N[t]\rangle = \mathcal{H}|\mathbb{P}_N[t]\rangle$, where $\mathcal{H}$ is the Hamiltonian that is derived based on the dynamics of the system [48]. For the other update rules, it is more convenient to use a "transfer matrix" $\mathcal{T}$ and consider $|\mathbb{P}_N[t+1]\rangle = \mathcal{T}|\mathbb{P}_N[t]\rangle$. For further details on the master equation and its formulation, we refer the reader to [27, 48].

The steady state $\lim_{t\to\infty}\Delta|\mathbb{P}_N(t)\rangle = 0$ for the random sequential TASEP is determined by the eigenstate of $\mathcal{H}$ that has an eigenvalue 0. Alternatively, if the transfer matrix formulation is used, its eigenstate with eigenvalue 1 gives the steady state. Solving for the steady state is a formidable task which may be accomplished by considering

recursion-based techniques on the system size [45, 46]. A more elegant and direct procedure however is to use a matrix product ansatz (MPA) [48], wherein the probability of each configuration at steady state is decomposed into a product of matrices.

Consider the unnormalized probabilities of the configurations at steady state, $f_N(\tau_1, \tau_2, \ldots, \tau_N)$, defined as

$$f_N(\tau_1, \tau_2, \ldots, \tau_N) = \mathbb{P}_N(\tau_1, \tau_2, \ldots, \tau_N) Z_N,$$

where

$$Z_N = \sum_{\tau_1 \in \{0,1\}} \sum_{\tau_2 \in \{0,1\}} \cdots \sum_{\tau_N \in \{0,1\}} f_N(\tau_1, \tau_2, \ldots, \tau_N)$$

is the partition function of the TASEP. According to the MPA, for each of the four TASEP updating procedures, it is possible to express $f_N(\tau_1, \tau_2, \ldots, \tau_N)$ as [27]

$$f_N(\tau_1, \tau_2, \ldots, \tau_N) = \langle W | \prod_{i=1}^{N} (\tau_i D + (1 - \tau_i) E) | V \rangle, \tag{3.3}$$

where $D$ and $E$ are square matrices that operate on occupied and empty sites, respectively, and $|V\rangle$ and $\langle W|$ are column and row vectors respectively (represented here by the "ket" and "bra" notation). From (3.3), we also see that $Z_N = \langle W | C^N | V \rangle$, with $C = D + E$.

Evidently, the elements of the matrices and vectors depend strongly on the updating procedure, and in general, they are infinite-dimensional [27]. Nevertheless, the MPA provides an analytical framework for describing the asymmetric exclusion process in a completely algebraic manner. Using this formalism, one can efficiently compute the steady state probabilities and, consequently, determine other physical quantities such as the moments and correlations of the site occupancies and the rate of flow of particles in the system.

3.5   Throughput and Delay Analysis for the r-TDMA-based Line Network

In this section, we characterize the steady state throughput and delay behavior of r-TDMA-based line networks. We also apply our results to studying the problem of short-hop-versus long-hop-routing. Recall that in the r-TDMA scheme, the transmitting node is chosen uniformly randomly in each time slot. Thus, observing that this scheme is analogous to the TASEP model with random sequential update, we can apply the results from the random sequential TASEP literature for our analysis.

In addition to the model described in Section 3.2, we assume that each node transmits at unit power, and that the channels are subject to Rayleigh fading. Thus, when node $i$ transmits, the received power at node $i + 1$ is exponentially distributed with mean $l^{-\gamma}$, where $\gamma$ is the path loss exponent. Since there is no interference in the network,

$$p_s = \Pr[\mathrm{SNR} > \Theta] = \exp\left(-\Theta N_0 l^\gamma\right). \tag{3.4}$$

Also, since the links are spaced equally, the success probability across any link is the same. This is equivalent to taking $\alpha = \beta = p = p_s$ in the corresponding TASEP model.

### 3.5.1 Steady State Probabilities

In the long time limit, the wireless network reaches a steady state where the probabilities $\mathbb{P}_N(\tau_1, \tau_2, \dots, \tau_N)$ of finding the system in the configurations $(\tau_1, \tau_2, \dots, \tau_N)$ are stationary (independent of $t$). It is proved in [48] that the matrices $D, E$ and vectors $V, W$ in (3.3) are in general, infinite-dimensional[1]. For $\alpha = \beta = p = p_s$ (which is the case in our system model), a simple choice of matrices and vectors (assuming $p_s > 0$) is

$$D = \frac{1}{p_s} \begin{pmatrix} 1 & 1 & 0 & 0 & \dots \\ 0 & 1 & 1 & 0 & \dots \\ 0 & 0 & 1 & 1 & \dots \\ 0 & 0 & 0 & 1 & \dots \\ \vdots & \vdots & \vdots & \vdots & \ddots \end{pmatrix} \quad \text{and} \quad E = D^T$$

with

$$\langle W| = (1, 0, 0, \dots) \quad \text{and} \quad |V\rangle = (1, 0, 0, \dots)^T.$$

Here, $(\cdot)^T$ indicates transposition.

Using (3.3), the steady state probabilities can be computed in a straightforward manner, in particular for small values of $N$. As examples, we have

$$f_1(0) = f_1(1) = 1/p_s,$$

and

$$f_2(0,0) = f_2(0,1) = f_2(1,1) = 1/p_s; \quad f_2(1,0) = 2/p_s.$$

---

[1] The only case for which the matrices are finite-dimensional (in fact, scalars) is when $\alpha + \beta = p$.

### 3.5.2 Steady State Occupancies

For any node $i$, its steady state occupancy is defined as the fraction of time it is occupied at steady state i.e., $\mathbb{P}(\tau_i = 1)$. In queueing-theoretic terms, the occupancy of site $i$ is the same as the *utilization factor* of the server at the $i^{\text{th}}$ node. Note that since $\tau_i$ can take values only in $\{0, 1\}$, we can also write $\mathbb{P}(\tau_i = 1) = \mathbb{E}\tau_i$ and $\mathbb{P}(\tau_i = 0) = 1 - \mathbb{E}\tau_i$. In a multihop line network with $N$ relays, the steady state occupancy of site $i$ is

$$\mathbb{E}\tau_{i,N} = \sum_{\tau_1 = \{0,1\}} \sum_{\tau_2 = \{0,1\}} \cdots \sum_{\tau_N = \{0,1\}} \tau_i f_N(\tau_1, \tau_2, \ldots, \tau_N)/Z_N. \tag{3.5}$$

Based on the MPA [48], this can be expressed as

$$\mathbb{E}\tau_{i,N} = \frac{\langle W | C^{i-1} D C^{N-i} | V \rangle}{\langle W | C^N | V \rangle}, \quad 1 \leq i \leq N. \tag{3.6}$$

Also note that since $\tau_0 = 1$, we have $\mathbb{E}\tau_{0,N} = 1$. In the rest of the chapter, we simplify the notation slightly wherever possible, and use $\mathbb{E}\tau_i$ to denote the occupancy of the $i^{\text{th}}$ site in the system with $N$ sites.

Using the forms of the matrices and vectors specified earlier, we see that in (3.6), both the numerator and the denominator contain a factor of $(1/p_s)^N$. Hence, the occupancies are independent of $p_s$. Therefore, to compute $\mathbb{E}\tau_i$, we can take $p_s = 1$, and the steady state occupancies are equivalent to those in [45, Eqn. 48], i.e.,

$$\mathbb{E}\tau_i = \frac{1}{2} + \frac{1}{4} \frac{(2i)!}{(i!)^2} \frac{(N!)^2}{(2N+1)!} \frac{(2N-2i+2)!}{[(N-i+1)!]^2}(N-2i+1). \tag{3.7}$$

The values at the end nodes are

$$\mathbb{E}\tau_1 = \frac{3N}{2(2N+1)} \quad \text{and} \quad \mathbb{E}\tau_N = \frac{N+2}{2(2N+1)}.$$

Fig. 3.4 shows the occupancies $\mathbb{E}\tau_i$ for a multihop network with 10 relay nodes. Notice the particle-hole symmetry i.e., $\mathbb{E}\tau_i = 1 - \mathbb{E}\tau_{N+1-i}$. In a system with an odd number of relays, the middle relay has an occupancy of exactly $1/2$.

*Asymptotics*: Taking the limit $N \to \infty$ for fixed $i$ in (3.7) yields

$$\mathbb{E}\tau_i = \frac{1}{2} + \frac{(2i)!}{(i!)^2} \frac{1}{2^{2i+1}}, \quad i \ll N. \tag{3.8}$$

In particular, $\mathbb{E}\tau_1 = 3/4$, and thus by the particle-hole symmetry, $\mathbb{E}\tau_N = 1/4$. Furthermore, for large $N$, the bulk of the system has an occupancy of approximately $1/2$ at steady state [45], i.e.,

$$\mathbb{E}\tau_i \approx 1/2 \quad \text{for} \quad i \gg 1, |i - N| \gg 1. \tag{3.9}$$
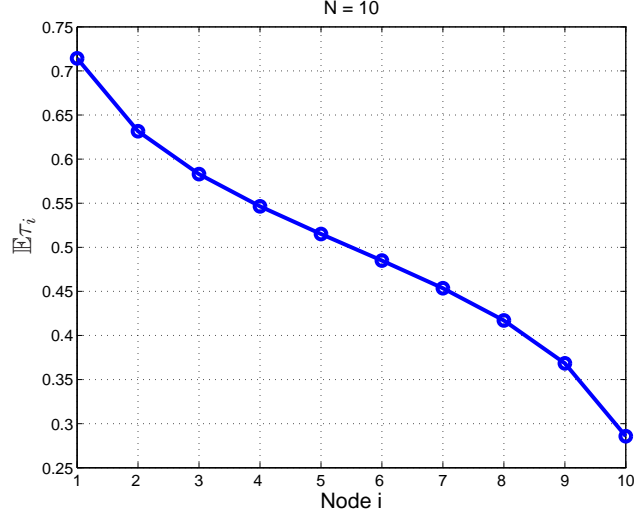
37

Figure 3.4. The steady state occupancy of each relay node for a r-TDMA-based multihop network with $N = 10$ relays. Notice the particle-hole symmetry $\mathbb{E}\tau_i = 1 - \mathbb{E}\tau_{N+1-i}$.

### 3.5.3  Steady State Throughput

At steady state, the rate of packet flow is the same over each link. The throughput (or current) through node $i$ is simply

$$T = p_s \frac{\mathbb{E}\left[\tau_i(1 - \tau_{i+1})\right]}{N + 1}, \tag{3.10}$$

because the probability that a packet successfully hops from node $i$ to $i + 1$ in a time step is $p_s\tau_i(1 - \tau_{i+1})/(N + 1)$. Using the MPA approach [48], we can write (3.10) as

$$T = \frac{p_s}{N + 1} \frac{\langle W|C^{i-1}DEC^{N-i-1}|V\rangle}{\langle W|C^N|V\rangle} = \frac{\langle W|C^{N-1}|V\rangle}{(N + 1)\langle W|C^N|V\rangle},$$

where the second equality holds since $p_s DE = D + E = C$. Using [48, Eqn. 80], this can be simplified to

$$T = \frac{A(N)p_s^N}{(N + 1)A(N + 1)p_s^{N-1}} = \frac{p_s(N + 2)}{2(N + 1)(2N + 1)}, \tag{3.11}$$

where $A(N) = p_s^{N-1}\langle W|C^{N-1}|V\rangle = \frac{(2N)!}{(N+1)!N!}$. Note that the throughput can also be computed using one of the two equivalent expressions, $T = p_s(1 - \mathbb{E}\tau_1)/(N + 1) = p_s\mathbb{E}\tau_N/(N + 1)$.

We comment that instead of picking one of the $N + 1$ nodes randomly, if one only chooses one of the nodes having a packet, the throughput is improved by a factor of $N + 1/(\sum_{i=0}^{N}\mathbb{E}\tau_i) = 2(N + 1)/N + 2$, i.e., $T = p_s/(2N + 1)$.

38

The system throughput at steady state is proportional to the link reliability and upper bounded by $p_s/4$, but decreases with increase in the system size: $T \sim p_s/(4N)$ for[2] $N \gg 1$. Intuitively, this result is understood by noting that only one node transmits in any time slot (in other words, the channel is not spatially reused), and this transmission is successful with probability $p_s/4$ (since both the transmitting and receiving nodes' buffers are each occupied independently with probability $1/2$).

3.5.4   Average End-to-End Delay at Steady State

In this section, we analyze the delay experienced at each node in the network (source and relays) and compute the average end-to-end delay for a packet at steady state.

**Theorem 3.5.1.** *For the wireless multihop network with $N$ relays running the r-TDMA scheme, the delay experienced by a packet at node $i$ follows a geometric distribution with mean*

$$\mathbb{E}D_i = \frac{2(N+1)(2N+1)\mathbb{E}\tau_i}{(N+2)p_s}, \quad 0 \le i \le N. \tag{3.12}$$

*Also, the average end-to-end delay is given by*

$$\mathbb{E}D_{e2e} = \frac{2N^2 + 3N + 1}{p_s}. \tag{3.13}$$

*Proof:*   Suppose that a packet arrives at an arbitrary node $i$, $0 \le i \le N$. The three events that need to occur in the following order for the packet to be able to hop to node $i + 1$ successfully are

(1) Node $i + 1$ has an empty buffer.

(2) Node $i$ is picked for transmission.

(3) Node $i$'s transmission is successful.

We first compute the probability that event (1) occurs, i.e., the node $i + 1$'s buffer is empty, conditioned on the fact that there is a packet present in node $i$'s buffer. This will help us determine the packet at the $i^{\text{th}}$ node can hop or not. We have

$$
\begin{aligned}
\mathbb{P}(\tau_{i+1} = 1 | \tau_i = 1) &= \frac{\mathbb{P}(\tau_{i+1} = 1, \tau_i = 1)}{\mathbb{P}(\tau_i = 1)} \\
&\overset{(a)}{=} \frac{\mathbb{E}[\tau_i \tau_{i+1}]}{\mathbb{E}\tau_i} \\
&\overset{(b)}{=} \frac{\mathbb{E}\tau_i - T(N+1)/p_s}{\mathbb{E}\tau_i} \\
&= 1 - \frac{N+2}{2(2N+1)\mathbb{E}\tau_i}, \tag{3.14}
\end{aligned}
$$

[2]The notation $f(n) \sim g(n)$ means that the ratio $f(n)/g(n)$ approaches 1 asymptotically (as $n \to \infty$).

39

where $(a)$ holds because $(\tau_i, \tau_{i+1})$ can only take values in $\{(0,0), (0,1), (1,0), (1,1)\}$ and $(b)$ is obtained by manipulating (3.10). Thus, we obtain

$$\mathbb{P}(\tau_{i+1} = 0 | \tau_i = 1) = \frac{N+2}{2(2N+1)\mathbb{E}\tau_i}. \tag{3.15}$$

Now, once event (1) occurs, $1/(N+1)$ is the probability of node $i$ being picked in the r-TDMA scheme, and after the occurrence of event 2), event 3) occurs with probability $p_s$. Therefore, in any time slot, the probability $p'$ of the packet at $i$ hopping is

$$p' = \frac{N+2}{2(2N+1)\mathbb{E}\tau_i} \cdot \frac{1}{N+1} \cdot p_s.$$

Thus, the delay at node $i$, $D_i$ follows a geometric distribution with parameter $p'$. The average end-to-end delay is simply the sum of the average delays experienced at each node in the network. $\qquad\square$

We see that the average end-to-end delay is proportional to the mean site occupancies, and inversely proportional to the link reliability. Also, it is interesting to note that the product of throughput and average delay is $1 + N/2$, and is independent of $p_s$.

For large $N$, we immediately see from (3.13) that

$$\mathbb{E}D_{\text{e2e}} \sim \frac{2N^2}{p_s}. \tag{3.16}$$

The average end-to-end delay grows quadratically with the number of relay nodes $N$.

3.5.5   End-to-End Delay for the First Packet

We now present a basic, yet useful result on the transient behavior of the r-TDMA-based multihop network. Specifically, we determine the pdf of the end-to-end delay experienced by the first transmitted packet. Evidently, the average end-to-end delay for any packet is lower and upper bounded by the average end-to-end delay for the first packet and the average steady state end-to-end delay, respectively.

**Corollary 3.5.2.** *For the wireless multihop network with $N$ relays running the r-TDMA scheme, the end-to-end delay experienced by the first transmitted packet follows a negative binomial distribution with parameters $N+1$ and $p_s/(N+1)$.*

*Proof:* When the first packet is transmitted, all the sites are empty. Equivalently, this means that upon the arrival of the packet at any node, the adjacent node has an empty buffer. Thus, for each $i \in \{0, 1, \ldots, N\}$, $D_i$ is geometrically distributed with mean $(N+1)/p_s$. Furthermore, since the $D_i$'s are independent for the first transmitted

packet, $D_{\mathrm{e2e}}$ is given by a negative binomial distribution with parameters $N+1$ and $p_s/(N+1)$. $\qquad\square$

The average end-to-end delay for the first packet is

$$\mathbb{E}D_{\mathrm{e2e}}^{\mathrm{f}} = \frac{(N+1)^2}{p_s}. \qquad (3.17)$$

From (3.13) and (3.17), we obtain

$$\frac{\mathbb{E}D_{\mathrm{e2e}}}{\mathbb{E}D_{\mathrm{e2e}}^{\mathrm{f}}} = \frac{N+1}{2N+1}.$$

For large $N$, $\mathbb{E}D_{\mathrm{e2e}} \approx 0.5\mathbb{E}D_{\mathrm{e2e}}^{\mathrm{f}}$.

Fig. 3.5 shows the theoretical value of the average end-to-end delay at steady state (3.13) and compares it with the average delay for the first packet (3.17) for $N = 10$. The empirical value of the average end-to-end delay for the second packet is also plotted, and it is seen to lie within the other two lines.
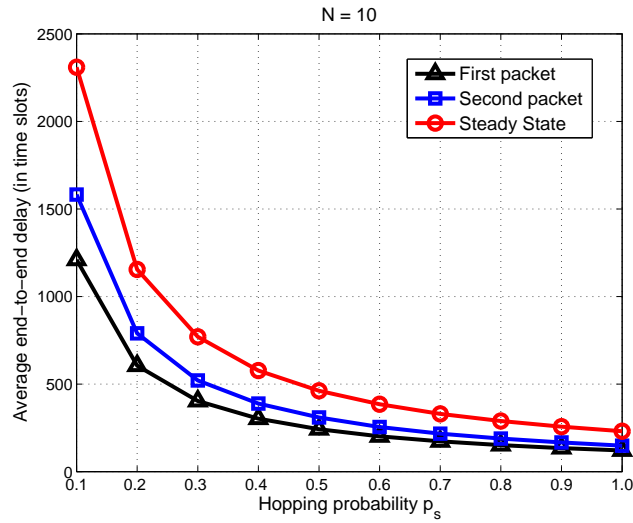


Figure 3.5. The average end-to-end delay of a packet at steady state and the same for the first transmitted packet for a r-TDMA-based multihop line network with 10 relays. The empirical value of the average end-to-end delay for the second transmitted packet is also shown, and as expected, it lies within the two other lines.

### 3.5.6 Spatial Delay Correlations

Since the packet flow in a wireless multihop network is relayed across multiple links, the delays experienced by a packet across hops are spatially correlated[3]. The correlation

---

[3]We like to remark that there also exists temporal correlations in the delay, which refers to the correlation between the delays experienced by two consecutive packets that arrived at a node. However,

coefficient between the delay at nodes $i$ and $j$ is defined as

$$\rho_{i,j} = \frac{\mathbb{E}\left[(D_i - \mathbb{E}[D_i])\,(D_j - \mathbb{E}[D_j])\right]}{\sigma_{D_i}\sigma_{D_j}}.$$

The study of delay correlations is important since it helps determine the variance of the end-to-end delay.

We now present some analytical results on the spatial delay correlations at steady state. Specifically, we compute $\mathbb{P}(D_{i+1} = n_{i+1}|D_i = n_i)$, i.e., given that at steady state, a packet stayed at node $i$ for $n_i$ slots, what is the probability that it will stay at node $i+1$ for $n_{i+1}$ slots? In the following, we derive closed-form expressions for the spatial delay correlations in multihop systems with $N = 1, 2$ relays, and also present some useful results in more general networks.

**Lemma 3.5.3.** *For the multihop wireless network with a single relay node, $D_0$ and $D_1$ are independent.*

*Proof:* For the trivial case $N = 1$, $\mathbb{P}(\tau_2 = 0) = 1$ by definition, and hence, irrespective of the packet delay at node 0, the packet can hop from node 1 to the destination (node 2) if node 1 is picked for transmission, and its transmission is successful. Thus, $D_1$ follows a geometric distribution with parameter $p_s/2$, and is independent of $D_0$, which is also geometrically distributed, but with parameter $p_s/4$ (3.12). $\qquad\square$

**Corollary 3.5.4.** *In a multihop wireless network with $N$ nodes, $D_N$ is independent of all the other hop delays.*

*Proof:* This is an immediate consequence of the previous lemma. Equivalently, we can state that the delay at any node $i$ is independent of the other delays in the network if $D_i$ follows a geometric distribution with parameter $p_s/(N+1)$. $\qquad\square$

Therefore, for $0 \le i \le N-1$, we have

$$\begin{aligned}
\mathbb{P}(D_N = n_N \mid D_i = n_i) &= \mathbb{P}(D_N = n_N) \\
&= \left(1 - \frac{p_s}{N+1}\right)^{n_N - 1} \frac{p_s}{N+1}.
\end{aligned}$$

A weaker statement is saying that $D_N$ is uncorrelated with the other delays, i.e., $\forall i$, $\rho_{i,N} = 0$, which is confirmed later in Fig. 3.7.

For $N > 1$, computing the spatial delay correlations is quite a formidable task. We now evaluate for $N = 2$, and the same procedure can be extended (with extra care) to

in this work, we characterize only the spatial delay correlations for a single packet.

evaluate the delay correlations for larger $N$. To make our analysis less cumbersome, we introduce the following notation.

(i) Let $E_i^{r,s}$ denote the event that when a packet arrives at node $i$, the configurations of the adjacent two sites are $(\tau_{i+1}, \tau_{i+2}) = (r, s)$, with $r, s \in \{0, 1\}$. Also, let $e_i^{r,s}(N) = \mathbb{P}(E_i^{r,s}) = \mathbb{P}((\tau_{i+1}, \tau_{i+2}) = (r, s) | \tau_i = 1)$.

Using the MPA, we have

$$
\begin{aligned}
e_i^{0,0}(N) \;\overset{(a)}{=}\;& \frac{\langle W | C^{i-1} D E E C^{N-i-2} | V \rangle}{\langle W | C^N | V \rangle} \\
\overset{(b)}{=}\;& \frac{\langle W | C^i E C^{N-i-2} | V \rangle}{p_s \langle W | C^N | V \rangle} \\
=\;& \frac{\langle W | C^i E C^{N-i-2} | V \rangle}{p_s \langle W | C^{N-1} | V \rangle} \frac{\langle W | C^{N-1} | V \rangle}{\langle W | C^N | V \rangle} \\
\overset{(c)}{=}\;& (1 - \mathbb{E}\tau_{i+1, N-1}) \frac{A(N)}{A(N+1)} \\
=\;& (1 - \mathbb{E}\tau_{i+1, N-1}) \frac{N+2}{2(2N+1)},
\end{aligned}
\tag{3.18}
$$

where $(a)$ is obtained using (3.3), $(b)$ using $p_s DE = D + E = C$, and $(c)$ using [49, Eqn. 80]. By a similar procedure, we obtain

$$
\begin{aligned}
e_i^{0,1}(N) \;=\;& \frac{\langle W | C^i D C^{N-i-2} | V \rangle}{p_s \langle W | C^{N-1} | V \rangle} \frac{\langle W | C^{N-1} | V \rangle}{\langle W | C^N | V \rangle} \\
=\;& \mathbb{E}\tau_{i+1, N-1} \frac{N+2}{2(2N+1)},
\end{aligned}
\tag{3.19}
$$

and

$$
\begin{aligned}
e_i^{1,0}(N) \;=\;& \frac{\langle W | C^{i-1} D D E C^{N-i-2} | V \rangle}{\langle W | C^N | V \rangle} \\
=\;& \frac{\langle W | C^{i-1} D C^{N-i-1} | V \rangle}{p_s \langle W | C^{N-1} | V \rangle} \frac{\langle W | C^{N-1} | V \rangle}{\langle W | C^N | V \rangle} \\
=\;& \mathbb{E}\tau_{i, N-1} \frac{N+2}{2(2N+1)}.
\end{aligned}
\tag{3.20}
$$

Since the probabilities of the events add up to $\mathbb{E}\tau_i$ (i.e., $\mathbb{E}\tau_{i,N}$), we get

$$
\begin{aligned}
e_i^{1,1}(N) \;=\;& \mathbb{E}\tau_{i,N} - e_i^{1,0}(N) - e_i^{0,1}(N) - e_i^{0,0}(N) \\
=\;& \mathbb{E}\tau_{i,N} - (1 + \mathbb{E}\tau_{i,N-1}) \frac{N+2}{2(2N+1)}.
\end{aligned}
\tag{3.21}
$$

(ii) Also, let

$$
g_N(k, l) = \begin{cases} (1 - p_s/(N+1))^k \, (p_s/(N+1))^l & l, k \geq 0 \\ 0 & \text{otherwise,} \end{cases}
$$

43

which has the following interesting property:

$$\prod_{i=1}^{n} g_N(k_i, l_i) = g_N\left(\sum_{i=1}^{n} k_i, \sum_{i=1}^{n} l_i\right) \quad \text{if } \forall i, k_i, l_i \geq 0. \tag{3.22}$$

**Theorem 3.5.5.** *For a multihop wireless network with $N = 2$ relays, we have*

$$\mathbb{P}(D_1 = n_1 \mid D_0 = n_0) = g_2(n_1 - 1, 1) - \frac{1}{5}\left(1 - \frac{2p_s}{3}\right)\left[g_2(n_0 + n_1 - 3, 1) + \right.$$

$$\left. 2(n_0 - 1)\frac{g_2(n_0 + n_1 - 4, 2)}{1 - g_2(n_0 - 1, 0)} + (n_0 - 2)\frac{g_2(n_0 + n_1 - 5, 2)}{1 - g_2(n_0 - 2, 0)}\right]. \tag{3.23}$$

*Proof:* When the packet under consideration arrives at node 0, let $(\tau_1', \tau_2')$ denote the configuration of the sites 1 and 2. For $N = 2$, we have from (3.18)-(3.21), $e_0^{0,0}(2) = 1/5$, $e_0^{0,1}(2) = 1/5$, $e_0^{1,0}(2) = 2/5$ and $e_0^{1,1}(2) = 1/5$. For the sake of notational convenience, let $p^{r,s}(n_0) = \mathbb{P}(D_1 = n_1 | D_0 = n_0, (\tau_1', \tau_2') = (r, s))$.

**Case 1:** $(\tau_1', \tau_2') = (0, 0)$.

In this case, $D_1$ is independent of $D_0$. Thus,

$$p^{0,0}(n_0) = g(n_1 - 1, 1). \tag{3.24}$$

**Case 2:** $(\tau_1', \tau_2') = (0, 1)$.

(i) If the delay experienced by the packet present at node 2 is smaller than $n_0$, node 2's buffer will be empty when the packet under consideration arrives at node 1, and thus, $D_1$ is again independent of $D_0$. This event occurs with probability

$$\sum_{k=0}^{n_0-2}\left(\frac{p_s}{3}\right)\left(1 - \frac{p_s}{3}\right)^k = 1 - \left(1 - \frac{p_s}{3}\right)^{n_0-1} = 1 - g(n_0 - 1, 0).$$

(ii) Thus, with probability $g(n_0 - 1, 0)$, the packet at node 2 remains there for more than $n_0$ slots. In this case, $\mathbb{P}(D_1 = n_1)$ is the probability that two successful transmissions (first of the packet at node 2 to the destination, and then of the packet at node 1 to (the then empty) node 2) occur in exactly $n_1 \geq 2$ slots, and is equal to

$$\left(1 - \frac{p_s}{3}\right)^{n_1-2}\left(\frac{p_s}{3}\right)^2 = g(n_1 - 2, 2).$$

Putting together the cases (i) and (ii), we have

$$p^{0,1}(n_0) = (1 - g(n_0 - 1, 0))g(n_1 - 1, 1) + g(n_0 - 1, 0)g(n_1 - 2, 2)$$

$$= g(n_1 - 1, 1) - g(n_0 + n_1 - 2, 1) + g(n_0 + n_1 - 3, 2)$$

$$= g(n_1 - 1, 1) - g(n_0 + n_1 - 3, 1)(1 - 2p_s/3). \tag{3.25}$$

44

**Case 3:** $(\tau_1', \tau_2') = (1, 0)$.

Since $D_0 = n_0$, the packet at node 1 has to hop to node 2 in $1 \leq l \leq n_0 - 1$ time slots. After this happens, this case is equivalent to case 2, with $n_0$ replaced by $n_0 - l$. Thus, we have

$$
\begin{aligned}
p^{1,0}(n_0) &= \frac{\sum_{l=1}^{n_0-1} \left(1 - \frac{p_s}{3}\right)^{l-1} \frac{p_s}{3} p^{0,1}(n_0 - l)}{\sum_{l=1}^{n_0-1} \left(1 - \frac{p_s}{3}\right)^{l-1} \frac{p_s}{3}} \\
&= \frac{\sum_{l=1}^{n_0-1} g(l-1,1) p^{0,1}(n_0 - l)}{1 - g(n_0 - 1, 0)} \\
&= g(n_1 - 1, 1) - \\
&\quad \frac{(n_0 - 1)(1 - 2p_s/3) g(n_0 + n_1 - 4, 2)}{1 - g(n_0 - 1, 0)}.
\end{aligned}
\tag{3.26}
$$

**Case 4:** $(\tau_1', \tau_2') = (1, 1)$.

Since $D_0 = n_0$, we require two successful transmissions (of the packets at nodes 2 and 1 to the destination and node 2 respectively) to occur in $2 \leq l \leq n_0 - 1$ slots. After this happens, this scenario is equivalent to case 2, with $n_0$ replaced by $n_0 - l$. Thus, we obtain

$$
\begin{aligned}
p^{(1,1)}(n_0) &= \frac{\sum_{l=2}^{n_0-1} \left(1 - \frac{p_s}{3}\right)^{l-2} \left(\frac{p_s}{3}\right)^2 p^{0,1}(n_0 - l)}{\sum_{l=2}^{n_0-1} \left(1 - \frac{p_s}{3}\right)^{l-2} \left(\frac{p_s}{3}\right)^2} \\
&= \frac{\sum_{l=2}^{n_0-1} g(l-2,1) p^{0,1}(n_0 - l)}{1 - g(n_0 - 2, 0)} \\
&= g(n_1 - 1, 1) - \\
&\quad \frac{(n_0 - 2)(1 - 2p_s/3) g(n_0 + n_1 - 5, 2)}{1 - g(n_0 - 2, 0)}.
\end{aligned}
\tag{3.27}
$$

Now, note that for case 1, $\mathbb{P}(D_1 = n_1 \mid D_0 = n_0)$ is non-zero for any values of $n_0$ and $n_1$, i.e., when $n_0 + n_1 \geq 2$ (since by assumption $n_0 \geq 1, n_1 \geq 1$). Likewise, it can be seen that for cases 2, 3 and 4, $\mathbb{P}(D_1 = n_1 \mid D_0 = n_0) > 0$ only when $n_0 + n_1 \geq 3$, $n_0 + n_1 \geq 4$ and $n_0 + n_1 \geq 5$ respectively. Putting this together with (3.24) - (3.27), we can write

$$
\mathbb{P}(D_1 = n_1 \mid D_0 = n_0) = \frac{\sum_{r,s \in \{0,1\}} e_0^{r,s}(2) p^{r,s}(n_0) \mathbf{1}_{n_0 + n_1 \geq c}}{\mathbb{P}(\tau_0 = 1)},
$$

where $c = 2r + s + 2$. In the general case ($n_0 + n_1 \geq 5$), the above equation is equivalent to (3.23). The factor $1/\mathbb{P}(\tau_0 = 1)$ (which is equal to 1) is required since the entire analysis is conditioned on the event that a packet is present at node 0. $\qquad \square$

Fig. 3.6 plots $\mathbb{P}(D_1 = n_1 | D_0 = n_0)/\mathbb{P}(D_1 = n_1)$ for different values of $n_0$ and $n_1$ for a

network with 2 relays when $p_s = 0.8$. The delay correlation $\mathbb{E}[D_0 D_1]$ can be numerically evaluated using (3.23) along with (3.12).
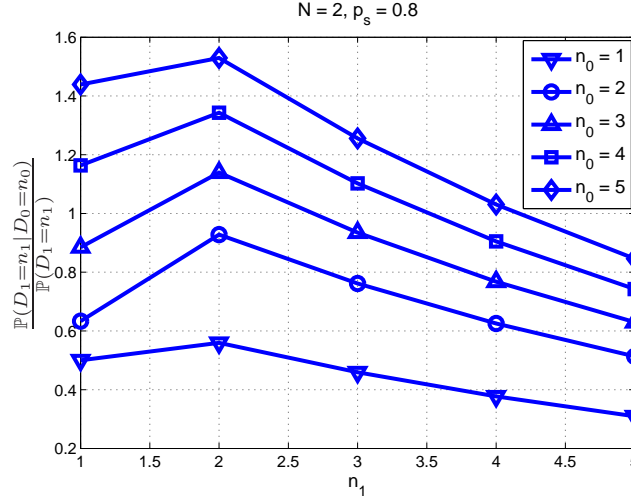


Figure 3.6. $\mathbb{P}(D_1 = n_1 | D_0 = n_0)/\mathbb{P}(D_1 = n_1)$ for different $n_0$ and $n_1$ for a multihop network with 2 relays.

**Corollary 3.5.6.** *For a multihop wireless network with $N$ relays, we have*

$$\mathbb{P}(D_{N-1} = n_{N-1} \mid D_{N-2} = n_{N-2}) = (\mathbb{E}\tau_{N-2})^{-1}\left[ g_N(n_{N-1} - 1, 1) - \left(1 - \frac{2p_s}{3}\right)\right( $$

$$e_{N-2}^{0,1}(N)g_2(n_0 + n_{N-1} - 3, 1) + e_{N-2}^{1,0}(N)(n_{N-2} - 1)\frac{g_N(n_{N-2} + n_{N-1} - 4, 2)}{1 - g_N(n_{N-2} - 1, 0)} + $$

$$e_{N-2}^{1,1}(N)(n_{N-2} - 2)\frac{g_N(n_{N-2} + n_{N-1} - 5, 2)}{1 - g_N(n_{N-2} - 2, 0)}\left)\right]. \ (3.28)$$

*Proof:* This is just a generalization of Theorem 3.5.5.                    $\square$

Evaluating the delay correlations for general $N$ or across farther nodes can be obtained by essentially following the same procedure, but gets computationally intensive and unwieldy. So, we resort to simulation. Fig. 3.7 plots the empirical values of delay correlations across one-, two- and three-hop neighbors in the r-TDMA-based wireless network with 10 relays and $p_s = 0.8$. First, observe that all the delay correlations are non-positive. This can be explained by noting that if the transmission of a packet is delayed at any node, the adjacent nodes' buffers get emptied so that the packet traverses faster across them. Likewise, if the waiting time of a packet at any particular node is small, the neighboring relay node buffers are still occupied and therefore it takes longer

for the packet to get transported across the system. Second, delays across hops closer to the destination and delays across father nodes are relatively lightly correlated. In fact, $\forall i$, $\rho_{i,N} = 0$. Therefore, much of the delay variance is actually contributed to only by the first few nodes near the source node.
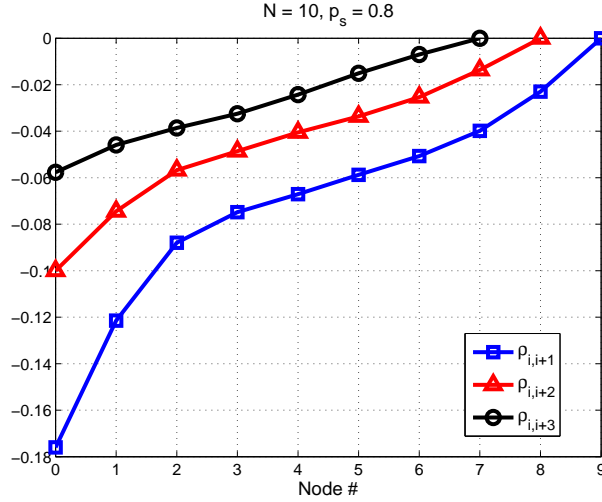


Figure 3.7. The correlation coefficients $\rho_{i,i+1}$, $\rho_{i,i+2}$ and $\rho_{i,i+3}$ for $p_s = 0.8$ in a multihop r-TDMA-based system with $N = 10$ relays. The delay correlations across nodes farther apart and closer to the destination are seen to be relatively light.

3.5.7   The Short-hop versus Long-hop Problem

We now present a simple application of the results derived so far: the short-hop versus long-hop problem in large regular wireless networks running the r-TDMA protocol. Specifically, we determine whether it is beneficial to route over many short hops or a smaller number of longer hops. The metrics we use for comparison are the average end-to-end delay and throughput.

Instead of considering all the $N$ nodes in the network, let us suppose that communication occurs only between nodes that are $m$ hops apart. Manipulating (3.4), it is straightforward to see that

$$p_s = \exp\left(-\Theta N_0 (ml)^\gamma\right).$$

We now determine the optimum spacing between the communicating hops, $m_{\mathrm{opt}}$, that minimizes the average end-to-end delay. For the system with $N/m$ relays (assuming that

$N$ is a multiple of $m$), we have

$$\mathbb{E}D_{e2e} \sim \frac{2(N/m)^2}{p_s} = 2N^2 \exp\left(\Theta N_0 (ml)^\gamma\right)/m^2, \tag{3.29}$$

Upon differentiating (3.29), we obtain

$$m_{\text{opt}} = \left(\frac{2}{\Theta N_0 l^\gamma \gamma}\right)^{1/\gamma}, \tag{3.30}$$

and is independent of $N$.

Fig. 3.8 plots the average end-to-end delay for different values of the SNR threshold for a system of length $N = 1000$ when $l = 1$. For each value of the threshold $\Theta$, observe that there is an optimum value of $m$ that minimizes the average end-to-end delay. The value of $m_{\text{opt}}$ (from (3.30)) for several values of $\gamma$ and $\Theta$ is plotted in Fig. 3.9. Depending on the threshold value, routing needs to be performed over longer or shorter hops in order to keep the packet delay minimal.
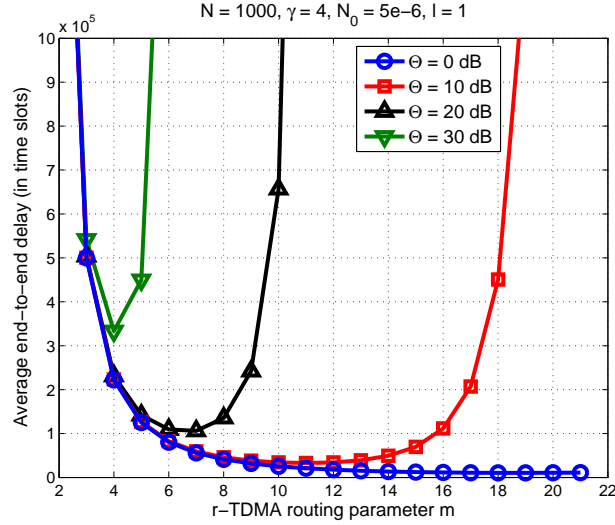


Figure 3.8. The average end-to-end delay versus the parameter $m$ for different values of threshold.

Likewise, let $m'_{\text{opt}}$ denote the optimum value of the spacing between hops for which the network throughput is maximized. We can express the throughput for the $N/m$-relay system as

$$T \sim \frac{p_s}{4N/m} = m \exp\left(-\Theta N_0 (ml)^\gamma\right)/4N \tag{3.31}$$
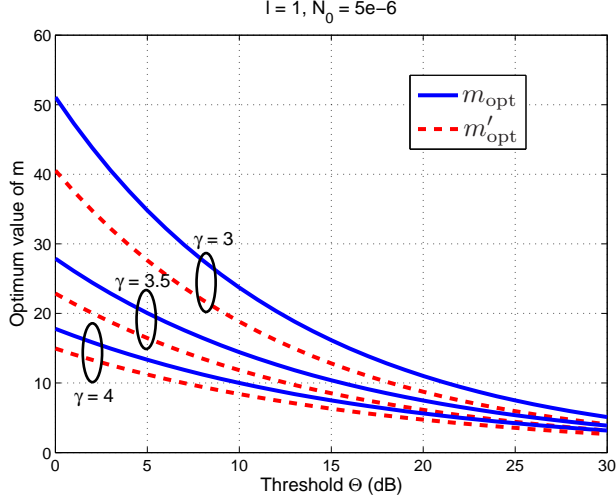
Figure 3.9. The values of the $m_{\text{opt}}$ and $m'_{\text{opt}}$ versus $\Theta$ for different values of the path loss exponent.

which is maximized at

$$m'_{\text{opt}} = \left( \frac{1}{\Theta N_0 l^\gamma \gamma} \right)^{1/\gamma}. \tag{3.32}$$

We see that $m_{\text{opt}}/m'_{\text{opt}} = 2^{1/\gamma}$. The values of $m'_{\text{opt}}$ are also depicted in Fig. 3.9.

## 3.6 Throughput and Delay for the Slotted ALOHA-based Line Network

In this section, we analyze the delay and throughput performance of slotted ALOHA-based wireless line networks with unit buffers at steady state. First, we consider the TASEP particle model with the parallel update and review some useful results. We then analytically compute the throughput and end-to-end delay for the TASEP system at steady state. Later, we consider a slotted ALOHA-based wireless large line network, analogize it to the particle model, and present another interesting application of the TASEP results.

### 3.6.1 Matrix and Vector Representation

Consider the TASEP particle flow model with the parallel update, and take the hopping probability to be equal to $p$ at all the sites, i.e., assume $\alpha = \beta = p$. In this section, we provide explicit representations of the matrices $D$ and $E$ and vectors $V$ and $W$ (see (3.3)) that help completely determine the probabilities of the steady state

configurations. When $\alpha = \beta = p$ (with $p > 0$), we have[4]

$$D = \begin{pmatrix} D_1 & 0 \\ D_2 & 0 \end{pmatrix}, \quad E = \begin{pmatrix} E_1 & E_2 \\ 0 & 0 \end{pmatrix},$$

$$\langle W| = (\langle W_1|, \langle W_2|) \quad, \quad |V\rangle = (|V_1\rangle, |V_2\rangle)^T,$$

where

$$D_1 = \begin{pmatrix} 1-p & \sqrt{1-p} & 0 & \dots \\ 0 & 1-p & \sqrt{1-p} & \dots \\ 0 & 0 & 1-p & \dots \\ \vdots & \vdots & \vdots & \ddots \end{pmatrix}, \quad E_1 = D_1^T,$$

$$\langle W_1| = (1, 0, 0, \dots) \quad, \quad |V_1\rangle = (1, 0, 0, \dots)^T,$$

and

$$E_2 = gD_1, D_2 = gE_1, \langle W_2| = g\langle W_1|, |V_2\rangle = g|V_1\rangle,$$

where $g = \sqrt{p/(1-p)}$.

Interestingly, in the limit $p \to 0$, the forms of the matrices for the parallel TASEP are identical to those obtained for the random sequential case (see Section 3.5.1), with $p_s = 1$. This can be intuitively understood by noting that by sufficiently reducing $p$, we can ensure that at most one transmission is successful. This way, we are emulating the TASEP model with random sequential update.

3.6.2   Buffer Occupancies

The average steady state occupancies are given by [49, Eqn. 10.16]

$$\mathbb{E}\tau_i = \frac{(1-p)\sum_{n=0}^{N-i} B(N-n)B(n) + pB(N)}{B(N+1) + pB(N)}, \tag{3.33}$$

where $B(0) = 1$, and

$$B(k) = \sum_{t=0}^{k-1} \frac{1}{k} \binom{k}{t} \binom{k}{t+1} (1-p)^t, \quad k > 0.$$

The steady state occupancies depend nontrivially on $p$ and are depicted in Fig. 3.10. Also, due to the particle-hole symmetry, we have $\mathbb{E}\tau_{\lceil (N+1)/2 \rceil} = \mathbb{E}\tau_{\lfloor (N+1)/2 \rfloor}$. For the case $p = 1$, the steady state configuration consists of alternating ones and zeros, and the occupancy of each relay node is exactly $1/2$.

---

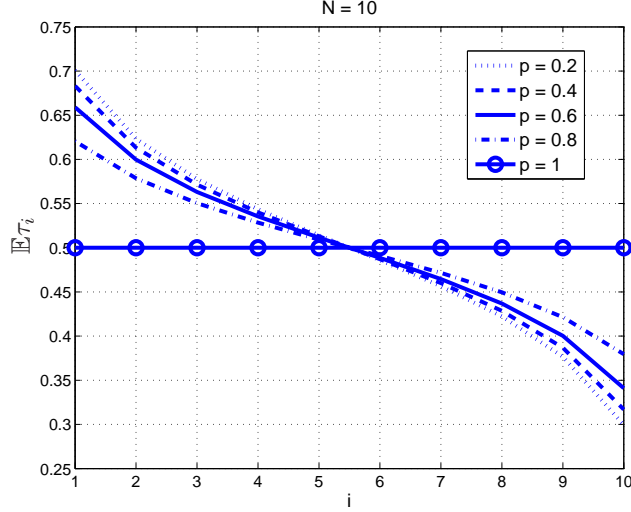[4]In general, the matrices are infinite-dimensional, unless $p = 1$ or $(1-\alpha)(1-\beta) = 1 - p$ [49].

Figure 3.10. The occupancies for the parallel TASEP-based particle flow model for different values of $p$. Unlike the r-TDMA case, $\mathbb{E}\tau_i$ critically depends on $p$. As $p \to 0$, the buffer occupancies approach those for the r-TDMA case.

*Asymptotics:* For large $N$, the steady state occupancy in the bulk is equal to $1/2$ [49], i.e., $\mathbb{E}\tau_i \approx 1/2$ for $i \gg 1$ and $|i - N| \gg 1$. Also, $\mathbb{E}\tau_1 = (2p - 1 + \sqrt{1-p})/2p$ and $\mathbb{E}\tau_N = (1 - \sqrt{1-p})/2p$.

### 3.6.3 Steady State Throughput

At steady state, the throughput (or current) through site $i$ is simply

$$T = p\mathbb{E}\left[\tau_i(1 - \tau_{i+1})\right],$$

because the probability that a particle successfully hops from node $i$ to $i + 1$ in a time step is $p\tau_i(1 - \tau_{i+1})$. At steady state, the rate of particle flow through each site is the same, and the throughput of the TASEP particle flow system is

$$T = p\mathbb{E}\tau_N = \frac{pB(N)}{B(N + 1) + pB(N)}. \tag{3.34}$$

For large $N$, the throughput at steady state $T \sim (1 - \sqrt{1-p})/2$ [49].

### 3.6.4 Steady State Delay

**Theorem 3.6.1.** *The delay $D_i$ experienced by a particle at node $i$ follows a geometric distribution, with mean*

$$\mathbb{E}D_i = \mathbb{E}\tau_i/(p\mathbb{E}\tau_N), \quad 0 \leq i \leq N. \tag{3.35}$$

51

*Proof:* Following the procedure described in 3.5.4, we can write the probability that the packet arriving at node $i$ hops successfully to node $i + 1$ in a time slot as

$$
\begin{aligned}
p' &= \mathbb{P}(\tau_{i+1} = 0 | \tau_i = 1) \cdot p \\
&= (1 - \mathbb{P}(\tau_{i+1} = 1 | \tau_i = 1)) \cdot p \\
&= \left(1 - \frac{\mathbb{P}(\tau_{i+1} = 1, \tau_i = 1)}{\mathbb{P}(\tau_i = 1)}\right) \cdot p \\
&\overset{(a)}{=} \left(1 - \frac{\mathbb{E}\tau_i - T/p}{\mathbb{E}\tau_i}\right) \cdot p = T/\mathbb{E}\tau_i \\
&\overset{(b)}{=} p\mathbb{E}\tau_N / \mathbb{E}\tau_i,
\end{aligned}
\tag{3.36}
$$

which is the same as (3.35). Here, $(a)$ holds since $T = p(\mathbb{E}\tau_i - \mathbb{E}[\tau_i\tau_{i+1}])$, and $(b)$ is from (3.34). $\qquad\square$

Consequently, the average end-to-end delay at steady state is obtained as

$$
\mathbb{E}D_{\text{e2e}} = \frac{1}{p\mathbb{E}\tau_N} \sum_{i=1}^{N} \mathbb{E}\tau_i = \frac{2N + 1}{2p\mathbb{E}\tau_N},
\tag{3.37}
$$

For large $N$, $\mathbb{E}D_{\text{e2e}} \sim (2N + 1)/(1 - \sqrt{1 - p})$.

Fig. 3.11 plots the mean end-to-end delay and throughput for a multihop line network with 10 relay nodes, running the slotted ALOHA protocol. As expected, the delays are much smaller than those observed in the r-TDMA-based line network (see Fig. 3.5). Also, as expected, $p = 1$ is the optimum value of the hopping probability for which the end-to-end delay is minimized, and the throughput is the highest. For this case, every second node transmits successfully in each time slot; the throughput is exactly equal to $1/2$, and the delay at each hope is equal to 1 time slot.

3.6.5   Spatial Delay Correlations

The delay correlations in the parallel TASEP-based system are harder to compute because of the stronger correlation between the site occupancies, thus, we only provide simulation results. Fig. 3.12 plots the empirical spatial correlations between the delays across different sites one hop, two hops and three hops apart in a 10-site system when $p = 0.8$. We again observe that the delay correlations are all negative and the correlations between the nearest sites close to the source contribute most to the spatial correlation. Also, note that the correlation curves are quite similar in shape to those for the r-TDMA-based wireless network (see Fig. 3.7).
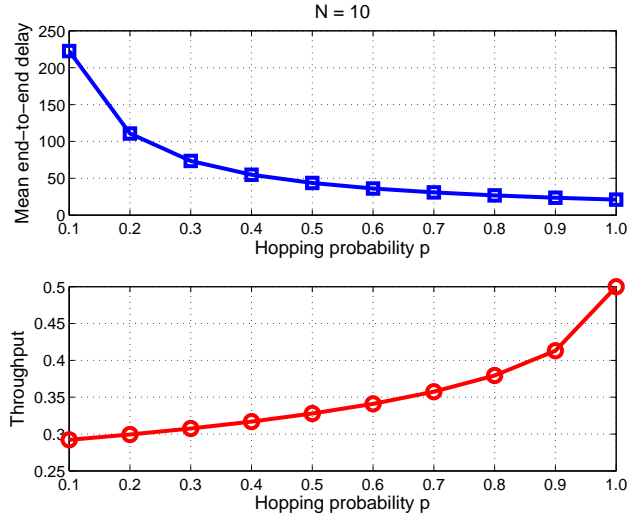
Figure 3.11. The average end-to-end delay and throughput for a parallel TASEP-based particle flow model with $N = 10$.

### 3.6.6 Optimizing the Contention Probability in Large ALOHA-based Line Networks

In this subsection, we analyze the throughput and average end-to-end delay of large ALOHA-based wireless networks (employing the modified transmission scheme) using results from the parallel TASEP. We also determine the optimum contention parameter for which the average delay across an arbitrary link is minimized.

We consider the line network model described in Section 3.2, and additionally assume that each node transmits at unit power, and that the channels are subject to Rayleigh fading. Let $\gamma$ denote the path loss exponent. Also, let $q$ denote the contention probability, i.e., in each time slot, nodes having a packet independently transmit with probability $q$ or stay idle with probability $1 - q$. Note the behavior of the delay across a link versus $q$. For small $q$, nodes hold on to packets for a long time before transmitting them which results in a long delay. Likewise, for large $q$, the interference in the network is high and the delay is large. An interesting question is to compute the optimum $q$ that minimizes the delay experienced by the packet across the link.

For analytical tractability, we employ the mean-field assumption [45], which is an approximation often used in statistical mechanics. Accordingly, the occupancies of the nodes are assumed to be uncorrelated i.e., $\forall i, j, \mathbb{E}[\tau_i \tau_j] = \mathbb{E}\tau_i \mathbb{E}\tau_j$. The mean-field as-
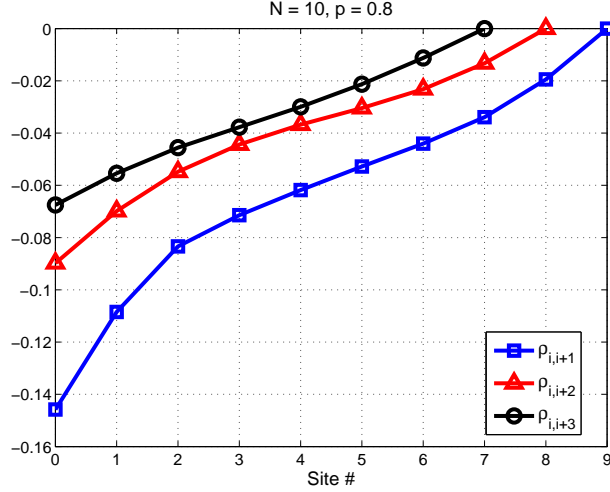
Figure 3.12. The empirical values of the correlation coefficients $\rho_{i,i+1}$, $\rho_{i,i+2}$ and $\rho_{i,i+3}$ for the TASEP model with parallel update. Here, $N = 10$ and $p = 0.8$.

sumption is tight at lower $p$ [49], and may be justified by considering high $\Theta$ or large interference from adjacent networks. Indeed, for adjacent nodes $i$ and $i + 1$, we have

$$\mathbb{P}(\tau_i = 1, \tau_{i+1} = 1) \quad = \quad \mathbb{E}[\tau_i \tau_{i+1}] = \mathbb{E}\tau_i - T/p.$$
$$\sim \quad 1/2 - (1 - \sqrt{1-p})/2p.$$

Now, when $p$ is small, $\sqrt{1-p} \approx 1 - p/2$; therefore $\mathbb{P}(\tau_i = 1, \tau_{i+1} = 1) \approx 1/4 \approx \mathbb{P}(\tau_i = 1)\mathbb{P}(\tau_{i+1} = 1)$, and the occupancies of nodes $i$ and $i + 1$ are independent of each other (and hence, uncorrelated).

We assume that the system is interference-limited and thus a transmission across any link is successful is the SIR at the receiver is greater than a threshold $\Theta$. Now, since each node is independently occupied with probability $1/2$, we can equivalently take the ALOHA contention parameter to be $q/2$. For the system model considered, the success probability is well-approximated by [50]

$$p \approx \exp(-qc), \tag{3.38}$$

where $c = \left( \pi \Theta^{1/\gamma} / \sqrt{\gamma/2} - 1 \right) / 2$.

Now, suppose that a packet arrives at an arbitrary node $i$ (with $i \gg 1$ and $|i - N| \gg 1$). It follows that the probability of a successful packet hop from node $i$ to $i + 1$ is $\approx qp/2$, because $\mathbb{P}(\tau_{i+1} = 0 | \tau_i = 1) = \mathbb{P}(\tau_{i+1} = 0) \approx 1/2$ and the probability of node $i$

transmitting the packet is $q$. Consequently, the average delay of the packet across the link $i \to i+1$ is

$$\begin{aligned} \mathbb{E}D_i &= 2/(qp) \\ &\approx 2 \exp\left(qc\right)/q. \end{aligned} \tag{3.39}$$

Differentiating (3.39), the optimum value of the contention parameter that minimizes the average delay across the link is obtained as

$$q_{\text{opt}} = \min\{1, 1/c\}. \tag{3.40}$$

Fig. 3.13 plots $q_{\text{opt}}$ versus threshold $\Theta$, for different path loss exponent values.
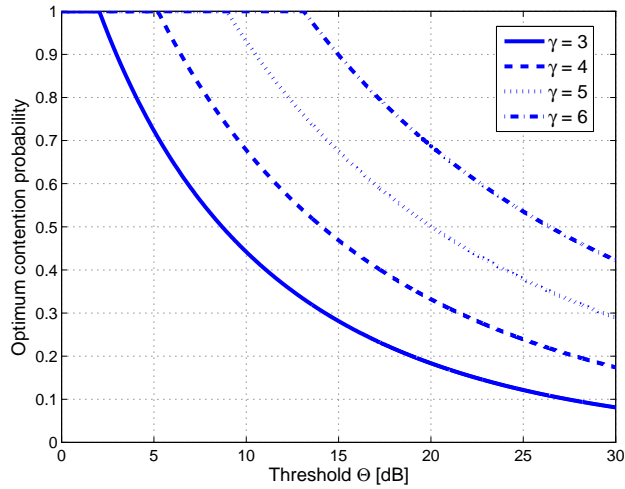


Figure 3.13. The optimum value of the contention parameter $q$ (that minimizes the delay across a link of length $l$) versus the SINR threshold $\Theta$ for different values of $\gamma$ in a large regular wireless network.

3.7   Chapter Summary and Concluding Remarks

We consider a wireless line network, where data is routed from the source to the destination in a multihop fashion. We propose a modified transmission policy that helps regulate the flow of packets in a completely decentralized manner. Using some known results from statistical mechanics, we characterize the end-to-end delay and throughput performances of multihop line networks running the r-TDMA and slotted ALOHA MAC

schemes. We extend the results derived to large networks and provide applications to important wireless networking problems.

The TASEP particle-flow model bridges the gap between statistical mechanics and wireless networking. It is useful for providing closed-form expressions for the average end-to-end delay and throughput of the multihop line network and has the advantage of obviating the cumbersome queueing theory-based analysis. Furthermore, the results obtained are scalable with the number of nodes and thus can provide helpful insights into the design of wireless networks.

CHAPTER 4

PROPOSED RESEARCH AND OPEN QUESTIONS

In this chapter, we describe the proposed research, and discuss several interesting open questions. The basic research goals are to analytically characterize (or at least provide upper and lower bounds to) the delay and throughput performance in a system of networks and to design appropriate routing protocols and network architectures that optimize the system performance. Additional objectives are to study the throughput-delay-reliability tradeoffs and to understand the transient behavior of multihop ad hoc networks.

These are some specific problems we would like to study:

4.1   Question 1: Routing Strategies in a System of Multihop Line Networks

We consider the problem of routing packets in a system of several multihop wireless line networks, which is both theoretically challenging and practically significant. Also, this framework is suitable for modeling ad hoc networks one since the aggregate flow in an ad hoc network can always be decomposed into several multihop line network flows. A preliminary, yet general formulation of the problem follows. We use some simplified assumptions in order to make the problem both tractable and interesting.

- Consider an ad hoc network where nodes designated to be source nodes are de-ployed on $\mathbb{R}^2$ as a homogeneous Poisson point process (PPP) with density $\lambda_s$. Additional nodes are arranged on $\mathbb{R}^2$ as a homogeneous PPP with density $\lambda - \lambda_s$. Thus, the total density of the network is $\lambda$. The PPP assumption may be justified by claiming that nodes may be dropped from aircraft in large numbers; for mobile ad hoc networks, it may be argued that terminals move independently from each other.

- Each source node decides to deliver packets to an arbitrarily chosen (destination) node that lies within a certain distance from the source node.

- For each source-destination pair, the route of packet flow is prescribed by a routing scheme $\mathcal{R}$, which basically selects a set of (relay) nodes involved in establishing the link[1]. Thus, the system can be perceived as comprising multiple multihop line networks.

- Time is slotted to the duration of a packet. In each time slot, the network MAC scheme $\mathcal{M}$ determines the set of transmitters for each of the line networks.

- We assume that nodes employ the revised transmission policy (described in Section 3.3.2). Thus, all the buffering is performed at the sources, and packets can hop only to nodes with empty buffers. Also, each relay node maintains a buffer of size unity for each of the line networks it is associated with.

- Links are subject to i.i.d. Rayleigh fading, and receptions are successful if the SINR at the receiver is greater than a threshold $\Theta$. It is assumed that each node transmits at unit power. Then the success probability across any link $x \rightarrow y$ (assuming the system is interference-limited) is

$$p_s = \mathbb{P}\left(\frac{h_{xy}g(x-y)}{I_{\Phi\backslash\{x\}}(y)} > \Theta\right), \tag{4.1}$$

where $g(x-y)$ is the large scale path loss function, typically of the form $g(x-y) = \|x-y\|^{-\gamma}$, and $h_{xy}$ is an exponentially distributed random variable representing the small-scale fading. Here, $I_{\Phi\backslash\{x\}}$ denotes the interference due to all transmitters in the network, except the intended transmitter at $x$.

### 4.1.1 Preliminary Results

We now provide some preliminary simulation-based results on the performance of the network that leads to some interesting questions. In particular, consider the following simple routing and MAC schemes:

$\mathcal{R}_1$: nearest-neighbor routing in a sector of angle $\phi$, i.e., the next-hop neighbor that lies within a sector of angle $\pm\phi/2$ to the destination (see Figure 4.1).

---

[1]In general, note that a node may be a part of multiple line networks.

$\mathcal{M}_1$: The r-TDMA scheme. For each line network, a node is uniformly randomly picked for transmission in a given time slot.
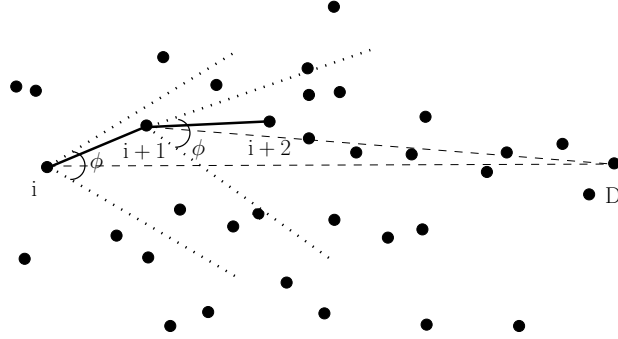


Figure 4.1. Illustration of nearest-neighbor routing in a sector of angle $\phi$. The packet is routed through nodes $i$, $i+1$ and $i+2$.

Figure 4.2 plots the attained throughput of the links at the end of 10000 time slots for different values of $\lambda_s$, in a network with $\lambda = 10$. Here, for the purpose of illustration, the destination node is taken to be 5 hops away from the source. The width of the lines represents the number of successfully transmitted packets across the link. Note than when $\lambda_s$ is very small, all transmissions may be simultaneously successful owing to smaller interference in the network, and this results in a reasonable sum through-put. With increasing $\lambda_s$, the number of source nodes is larger, and the throughput can be made larger. However, when $\lambda_s$ is very large, the interference in the network also increases resulting in a lower throughput, which is undesirable. The natural question to ask is: What is the optimum density of sources for which the sum throughput of the network is maximized? Answering this question requires characterizing the success probability across the links and then quantifying the throughput (current) in each net-work. Along similar lines, one may ask: what is the optimal value of $\lambda_s$ for which the average end-to-end delay of packets is minimized?

### 4.1.2 Prior Work

There is a significant body of prior work related to the aforementioned questions. For example, a problem of similar flavor is studied in [18] wherein the authors evaluate the optimal density of transmitters in interference-limited Poisson point processes that maximizes the expected progress of a packet. In [20], the authors examine the tradeoff
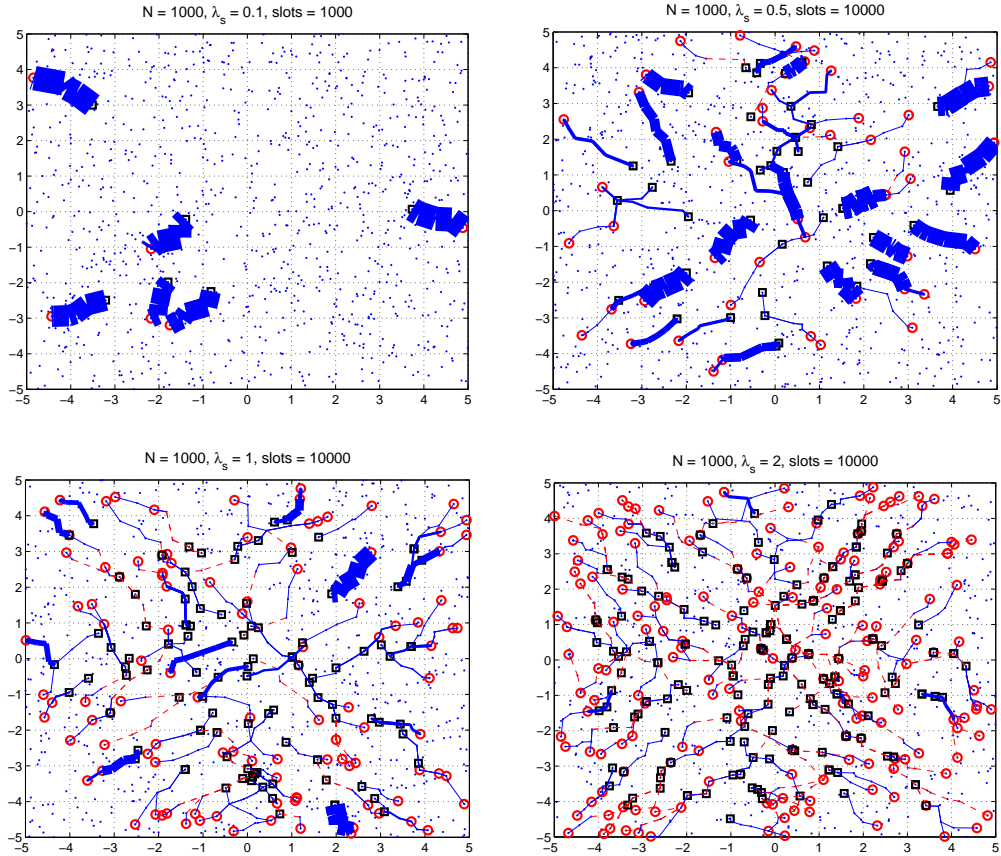
Figure 4.2. The sum throughput of the links for different values of $\lambda_s$ in a network with $\lambda = 10$ at the end of 10000 time slots. The red circles denote the source nodes while the black squares the destination nodes. The thickness of the solid (blue) lines is proportional to the number of successful transmissions across the link. The dashed (red) lines indicate that all packet transmissions across that link were unsuccessful. Among these plots, $\lambda_s = 0.5$ seems to perform the best in terms of sum throughput.

between increased transmission radius resulting in fewer hops to the destination, and the effective rate lost at each node as a result of the increase in transmission range. In [51], the authors evaluate the transmission capacity of wireless ad hoc networks, which is the maximum spatial density of successful transmissions such that the outage probability is lower than a specified threshold. However, even though problems of this nature are well-studied, in prior work, authors have neglected the queueing delays in the system, and assumed oversimplified system models in which nodes always have packets to transmit. To the best of our knowledge, this is the first attempt at analyzing this problem while taking into consideration the flow of packets in the network as well.

### 4.1.3 Pertinent Questions

Several related issues of theoretical and practical nature arise. For example:

1. For the routing and MAC schemes $\mathcal{R}_1$ and $\mathcal{M}_1$ respectively, how does one choose the value of $\phi$? Note that for small $\phi$, the packet has to hop over longer distances, while for large $\phi$, the progress of a packet towards its destination is small.

2. The long-hop versus short-hop problem: instead of hopping over nearest neighbors, does it benefit to hop over farther (say $m$) neighbors?

3. How to jointly optimize $\lambda_s$, $\phi$ and $m$ in order to maximize the sum throughput for a given $\mathcal{R}$ and $\mathcal{M}$? As a starting point, we can consider the routing and MAC schemes $\mathcal{R}_1$ and $\mathcal{M}_1$ respectively. For this setting, what is the scaling of the transport capacity with the network size? How do the results change when we consider other MAC schemes, such as slotted ALOHA or spatial TDMA?

4. Consider the issue of broadcasting with multiple sources. In this context, how fast do messages propagate in the network? Also, what are the properties of the paths formed (for example, what is the average number of hops traversed by a packet in a given time? How many different paths exist between two nodes? What is the path efficiency?)? This problem is similar in flavor to the one discussed in [52]. As a special case, if all sources have the same message to transmit, how fast can the system be flooded?

5. How do the results change when we consider 3 (or higher) dimensions, a different

underlying nodal distribution (e.g., a Manhattan grid) or a more general fading model (for example, Nakagami-$m$)?

## 4.2 Question 2: TDR Region Characterization of line networks

A more general question than the one described in the earlier section is the detailed characterization of the throughput-delay-reliability (TDR) region of a line network. Recall that in the revised transmission policy (Section 3.3.2), we set the reliability of the network to 100% by retransmitting packets whenever the reception fails. Also recall that for the r-TDMA-based network, the throughput is $p_s(N + 2)/\left(2(2N^2 + 3N + 1)\right)$ (3.11) and the average end-to-end delay is $(2N^2 + 3N + 1)/p_s$ (3.13). Therefore, TDR region is a hyperbolic curve along the unit-reliability plane, and the area above this curve represents the achievable or feasible region.

However, when the hopping probability is low, keeping reliability at 1 requires packets to be retransmitted several times and results in an unnecessarily large queueing delay and consequently, a low throughput. In scenarios where reliability is not too critical, one can instead decide to drop packets with a certain probability and this will help maintain the throughput at a reasonably good value. In order to quantify this benefit in throughput, it is critical to study the TDR tradeoffs and characterize the TDR region for the multihop wireless network. Determining the TDR tradeoffs also helps determine the error exponent of the system, which describes the rate of decrease of error as a function of delay/blocklength.

It should be noted that this problem is very similar in flavor to the problem of coupling the TASEP to Langmuir Kinetics (LK) (see [53, 54]). While the TASEP model deals with the flow of particles along a lattice, the LK model deals with the adsorption (at empty sites) and desorption (from occupied sites) kinetics of particles. The TASEP and LK can be considered as two of the simplest paradigms which contrast equilibrium and non-equilibrium dynamics and stationary states. Evidently, setting the absorption rate in the LK model to zero and supplementing it by the TASEP model, the dynamics of dropping packets in the multihop line network can be studied.

As a starting point, consider a multihop line network with $N$ relay nodes running the r-TDMA-based scheme. Let $p$ denote the hopping probability, and consider the case when $p$ is small ($p \ll 1$). Now, suppose that particles are dropped with a certain

probability $q$ which is independent of $p$, and also site-independent.

The evolution of the occupancy of site $i$, $0 < i < N$ takes the form

$$\Delta\tau_i[t] = p\tau_{i-1}[t](1 - \tau_i[t]) - p\tau_i[t](1 - \tau_{i+1}[t]) - q\tau_i[t], \tag{4.2}$$

where $\Delta\tau_i[t] = \tau_i[t+1] - \tau_i[t]$. Similar expressions can also be obtained for the sites at the boundary ($i = \{0, N\}$).

When the network is large, we can neglect correlation between site occupancies and use the *mean field* approximation[2]. Accordingly, we take $\mathbb{E}[\tau_i\tau_{i+1}] \approx \tau_i\mathbb{E}\tau_{i+1}$. At steady state ($t \to \infty$), one obtains

$$\lim_{t\to\infty} \Delta\mathbb{E}\tau_i(t) = 0 \Leftrightarrow p\mathbb{E}\tau_{i-1} - p\mathbb{E}\tau_{i-1}\mathbb{E}\tau_i + p\mathbb{E}\tau_i\mathbb{E}\tau_{i+1} = (p+q)\mathbb{E}\tau_i. \tag{4.3}$$

The node occupancies $\mathbb{E}\tau_i$ can be obtained numerically by simultaneously solving $N$ such equations.

There has been significant work in characterizing the delay, throughput and reliability tradeoffs in wireless networks. In [55], the authors derive the delays for the Gupta-Kumar and Grossglauser-Tse models, and describe practical schemes to achieve the optimal throughput-delay tradeoff. Using ideas from queueing theory, the authors in [56] analyze the delay-reliability tradeoff in delay-bounded networks. The optimal rate-reliability-delay tradeoff in networks with composite links has been studied in [57] based on the Klienrock independence assumption. While the independence assumption is approximate for networks with multiple flows, in line networks, the flows are correlated and it is critical to characterize the tradeoffs while taking into account the routing and MAC schemes, the link reliability and the buffer size all together.

Some related questions are:

1. Characterize the TDR region in the case when $q$ is site-dependent? In a multihop line network, packets are usually crowded more near the source, and the nodes closer to the destination are less busy (See Figure 3.4). Thus, it seems more optimal to use a $q$ whose value is higher at nodes closer to the source, and smaller farther away from the source.

2. Instead of dropping packets at a certain rate, a more practical approach would be

---

[2]This approximation is quite tight for large $N$ and small $p$.

to only drop packets that cannot be successfully transmitted even after a period of time (say, $T$ time slots). What is the TDR region for delay-bounded line networks?

3. How does $q$ being queue-state dependent change the TDR region?

## 4.3    Question 3: Statistical Mechanics of CSMA-based Wireless Networks

Another interesting problem we would like to study is the statistical mechanics of CSMA-based wireless networks. This problem was motivated by Hastings in [6]. Consider a set of nodes that communicate with each other in an ad hoc fashion. The location of the nodes can be arbitrary; however for exposition purposes, we take that the nodes are arranged as a Manhattan grid with unit grid length. We assume the channel access scheme to be CSMA and take the communication range of each node to be unity. Thus, when a node senses the channel to be free, it can establish a connection with one of its neighbors. Once a link is established (or becomes 'active'), the nodes that established the link can communicate data with each other bidirectionally and all other nodes in the ranges of node the two nodes have to remain silent. Generally, a link may become active only if none of the two nodes' neighbors are active (see Figure. 4.3).
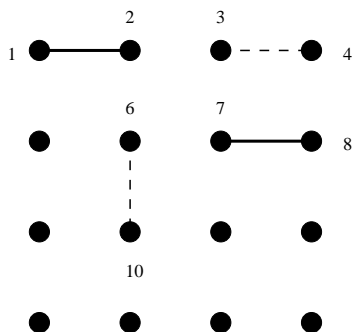


Figure 4.3. Illustration of CSMA-based communication in a Manhattan network. When nodes 1 and 2 form an active link, nodes 3 and 4 or nodes 6 and 10 cannot establish links with each other. However, nodes 7 an 8 can simultaneously communicate as well.

Now, assume that at each instant of time, each link that is inactive is activated at unit rate. This means that the time it takes an inactive link to be activated (provided that none of its neighbors are active) follows an exponential distribution with unit mean. Also, suppose that once a link is formed, the time it stays active follows an exponential distribution with rate $1/\rho$ (mean $\rho$), after which it becomes inactive. At $t = 0$, we assume
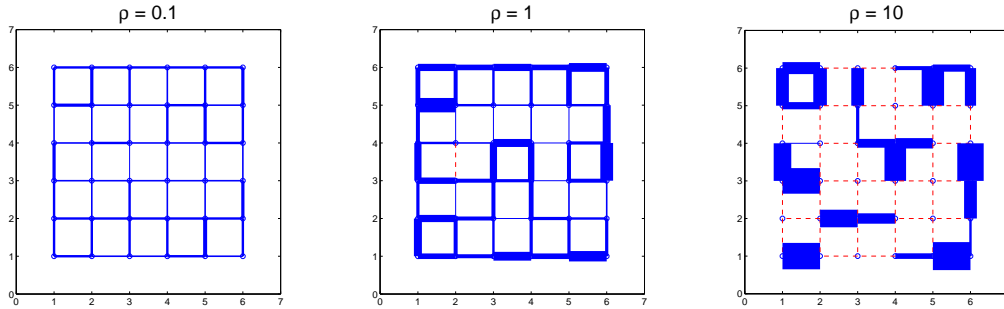
Figure 4.4. The throughput across the links in a $6 \times 6$ Manhattan network. The thickness of the lines is proportional to the time the links were active. The dashed lines indicate those nodes between which links weren't established. The tradeoff between $\rho$ and sum throughput is evident from the plots.

that there are no links present, and links get added and deleted as time progresses. Note the following tradeoffs. The larger $\rho$ is, links often become inactive and new links form. Thus, the average number of active links is larger, and the throughput is increased. However, if $\rho$ is very large, the system will get stuck in some configuration for a long period of time. This also prevents neighboring nodes from establishing connections, and the throughput is reduced.

Figure 4.4 plots the average throughput across the links of the Manhattan network for four different values of $\rho$, and clearly depicts the tradeoffs.

Several interesting questions arise:

1. What is the optimum $\rho$ for which the average sum throughput across a link is maximized? What is its value? Also, how does the optimum $\rho$ depend on the degree of the nodes? Note that the degree of the Manhattan network is 4.

2. Suppose node $i$ has a packet to transmit to node $j$. What is the probability that it is delivered at the end of $t$ time slots? How long does it take before the packet visits all the nodes? Is this question related to a random walk on integer lattices? There also seems to exist some natural correspondences between the flow of information in the CSMA-based Manhattan lattice and the issue of passage percolation, and it will be interesting to explore them.

3. It will be useful to understand the relationship between the Hastings and TASEP models.

65

## 4.4   Other Questions

1. Most of our results for the multihop line network have been derived under the steady state assumption, and thus only provide performance bounds. However, it is often the case that the time scales of operation is not large enough for the network to reach steady state. Thus, it is more important to characterize the transient behavior of the network, and address departures from the steady state behavior. A simple result in this direction has been to derive the delay pdf for the first transmitted packet (see Section 3.5.5).

2. Another challenging problem is to study the delay and throughput performance for different network topologies, such as ring networks, or tree networks. It might then be necessary to also consider bidirectional flow of traffic and periodic boundary conditions. Results and techniques from the ASEP or SSEP literature may be useful in studying this problem.

BIBLIOGRAPHY

[1] J. Andrews, N. Jindal, M. Haenggi, R. Berry, D. Guo, M. Neely, S. Weber, S. Jafar and A. Yener, "Rethinking information theory for mobile ad hoc networks," *IEEE Communications Magazine*, Vol. 46, pp. 94-101, Dec. 2008.

[2] A. Goldsmith and S. B. Wicker, "Design challenges for energy-constrained ad hoc wireless networks," *IEEE Wireless Communications Magazine*, Vol. 9, No. 4, pp. 8-27, Aug. 2002.

[3] R. C. Alamino and D. Saad, "Statistical mechanics analysis of LDPC coding in MIMO Gaussian channels," *Journal of Physics A: Mathematical and Theoretical*, Vol. 40, No. 41, pp. 12259-12279, Oct 2007.

[4] K. Takeuchi and T. Tanaka, "Statistical-mechanics-based analysis of multiuser MIMO channels with linear dispersion codes," *Journal of Physics: Conference Series*, Vol. 95, Iss. 1, Jan. 2008.

[5] D. Guo and S. Verdu, "Randomly spread CDMA: Asymptotics via statistical physics," *IEEE Transactions on Information Theory*, Vol. 51, pp. 1261-1282, Apr. 2005.

[6] M. B. Hastings, "Statistical mechanics of interfering links," *Physics Review E*, July 2005.

[7] M. Franceschetti and R. Meester, *Random Networks for Communication: From Statistical Physics to Information Systems*, Cambridge University Press, 2008.

[8] T. S. Rappaport, *Wireless Communications - Principles and Practice*, Prentice Hall, 1991.

[9] D. Stoyan, W. S. Kendall and J. Mecke, "Stochastic Geometry and its Applications," Wiley & Sons, 1978.

[10] L. E. Miller, "Distribution of link distance in a wireless network," *Journal of Research of National Institute of Standards and Technology*, Vol. 106, pp. 401-412, Mar./Apr. 2001.

[11] C. Rose, "Mean internodal distance in regular and random multihop networks," *IEEE Transactions on Communications*, Vol. 40, No. 8, pp. 1310-1318, Aug. 1992.

[12] M. Haenggi, "On distances in uniformly random networks," *IEEE Transactions on Information Theory*, Vol. 51, No. 10, pp. 3584-3586, Oct 2005.

[13] S. Vural and E. Ekici, Probability distribution of multihop distance in one-dimensional sensor networks, *Computer Networks Journal (Elsevier)*, Vol. 51, No. 13, pp. 3727-3749, Sep. 2007.

[14] L. E. Miller, "Joint distribution of link distances," *Conference on Information Sciences and Systems*, Mar. 2003.

[15] C-C. Tseng, H-T. Chen and K-C. Chen, "On the distance distributions of the wireless ad hoc networks," *IEEE Vehicular Technology Conference*, Vol. 2, pp. 772-776, May 2006.

[16] P. Kumaraswamy, "A generalized probability density function for double-bounded random processes," *Journal of Hydrology*, Vol. 46, No. 1/2, pp. 79-88, 1980.

[17] R. L. Graham, D. E. Knuth and O. Patashnik, "Concrete mathematics: A foundation for computer science," 2nd ed., Addison-Wesley, 1994.

[18] F. Baccelli, B. Błaszczyszyn and P. Mühlethaler, "An ALOHA protocol for multihop mobile wireless networks," *IEEE Transactions on Information Theory*, Vol. 52, No. 2, pp. 421-436, Feb. 2006.

[19] M. Haenggi, "On routing in random Rayleigh fading networks," *IEEE Transactions on Wireless Communications*, Vol. 4, No. 4, pp. 1553-1562, July 2005.

[20] H. Takagi and L. Kleinrock, "Optimal transmission ranges for randomly distributed packet radio terminals," *IEEE Transactions on Communications*, Vol. COM-32, No. 3, pp. 246-257, Mar. 1984.

[21] M. Haenggi and D. Puccinelli, "Routing in ad hoc networks: A case for long hops," *IEEE Communications Magazine*, Vol. 43, Iss. 10, pp. 93-101, Oct. 2005.

[22] M. Sikora, J. N. Laneman, M. Haenggi, D. J. Costello, and T. Fuja, "Bandwidth- and power-efficient routing in linear wireless networks," *Joint Special Issue of IEEE Transactions on Information Theory and IEEE Transactions on Networking*, Vol. 52, Iss. 6, pp. 2624-2633, June 2006.

[23] S. Srinivasa and M. Haenggi, "Path loss estimation in large wireless networks," in preparation for submission to *IEEE Transactions on Wireless Communications*. Available at `http://aps.arxiv.org/abs/0802.0351`.

[24] S. Xu and T. Saadawi, "Does the IEEE 802.11 MAC protocol work well in multihop wireless adhoc networks?," *IEEE Communications Magazine*, Vol. 36. Iss. 6, pp. 130-137, Jun 2001.

[25] Z. Fu, P. Zerfos, H. Luo, S. Lu, L. Zhang and M. Gerla, "The impact of multihop wireless channel on TCP throughput and loss," *INFOCOM 2003*, Vol. 3, pp. 1744-1753, Mar/Apr 2003.

[26] J. Li, C. Blake, D. S. J. De Couto, H. I. Lee, R. Morris, "Capacity of ad hoc wireless networks," *Proc. ACM International Conference on Mobile Computing and Networking*, pp. 61-69, Jul. 2001.

[27] N. Rajewsky, L. Santen, A. Schadschneider and M. Schreckenberg, "The asymmetric exclusion process: comparison of update procedures," *Journal of Statistical Physics*, Vol. 92, Nos. 1/2, pp. 151-194, Jul. 1998.

[28] L. Tassiulas, "Adaptive back-pressure congestion control based on local information," *IEEE Trans. on Automatic Control*, Vol. 40, No. 2, pp. 36-250, Feb. 1995.

[29] A. K. Elhakeem, R. Di Girolamo, I. B. Bdira, M. Talla, "Delay and throughput characteristics of TH, CDMA, TDMA, and hybrid networks for multipath faded data transmission channels," *IEEE Journal on Selected Areas in Communications*, Vol. 12, No. 4, pp. 622-637, May 1994.

[30] R. Nelson, L. Kleinrock, "Spatial TDMA: A collision-free multihop channel access protocol," *IEEE Transactions on Communications*, Vol. 33, No. 9, pp. 934-944, Sep. 1985.

[31] M. M. Carvalho and J. J. Garcia-Luna-Aceves, "Delay analysis of IEEE 802.11 in single-hop networks," *Proc. of the 11th IEEE International Conference on Network Protocols*, Iss. 4-7, pp. 146-155, Nov. 2003.

[32] S. L. Beuerman and E. J. Coyle, "The delay characteristics of CSMA/CD networks," *IEEE Transactions on Communications*, Vol. 36, No. 5, pp. 553-563, May 1988.

[33] M. Xie and M. Haenggi, "Towards an end-to-end delay analysis of wireless multihop networks," *Elsevier Ad Hoc Networks*, Vol. 7, pp. 849-861, July 2009.

[34] M. Xie and M. Haenggi, "A Study of the correlations between channel and traffic statistics in multihop networks," *IEEE Transactions on Vehicular Technology*, Vol. 56, pp. 3550-3562, Nov. 2007.

[35] N. Bisnik and A. A. Abouzeid, "Queuing network models for delay analysis of multihop wireless ad hoc networks," *Elsevier Ad Hoc Networks*, Vol. 7, Iss. 1, pp. 79-97, Jan. 2009.

[36] N. Ryoki, K. Kawahara, T. Ikenaga and Y. Oie, "Performance analysis of queue length distribution of tandem routers for QoS measurement," *Proc. IEEE Symposium on Applications and the Internet*, pp. 82-87, Jan. - Feb. 2002.

[37] M. Conti, E. Gregori and I. Stavrakakis, "Large impact of temporal/spatial correlations on per-session performance measures: single and multiple node cases," *Elsevier Performance Evaluation*, Vol. 41, No. 2-3, pp. 83-116, Jul. 2000.

[38] A. Bader and E. Ekici, "Throughput and delay optimization in interference-limited multi-hop networks," *Proc. ACM International Symposium on Mobile Ad Hoc Networking and Computing*, pp. 274-285, May 2006.

[39] P. Gupta and P. R. Kumar, "The capacity of wireless networks," *IEEE Transactions on Information Theory*, Vol. 46, Iss. 2, pp. 388-404, Mar. 2000.

[40] M. Grossglauser and D. N. C, Tse, "Mobility increases the capacity of ad hoc wireless networks," *IEEE Transactions on Information Theory*, Vol. 10, No. 4, p. 477-486, Aug. 2002.

[41] J. Abouei, A. Bayesteh, and A. K. Khandani, "Delay-throughput analysis in decentralized single-hop wireless networks," *IEEE Symposium on Information Theory*, 2007.

[42] Y. Yang and T. S. P. Yum, "Delay distributions of slotted ALOHA and CSMA," *IEEE Transactions on Communications*, Vol. 51, No. 11, pp. 1846-1857, Nov. 2003.

[43] O. Dousse, "Revising buffering in CSMA/CA wireless multihop networks," *Proc. SECON*, San Diego, June 2007.

[44] S. Bhadra and S. Shakkottai, "Looking at large networks: coding vs. queueing," *IEEE INFOCOM*, Apr. 2006.

[45] B. Derrida, E. Domany and D. Mukamel, "An exact solution of a one-dimensional asymmetric exclusion model with open boundaries," *Journal of Statistical Physics*, Vol. 69, Nos. 3/4, pp. 667-687, Nov. 1992.

[46] G. Schütz and E. Domany, "Phase transitions in an exactly soluble one-dimensional exclusion process," *Journal of Statistical Physics*, Vol. 72, Nos. 1/2, pp. 4265-4277, Jul. 1993.

[47] K. Nagel and M. Schreckenberg, "A cellular automaton model for freeway traffic," *Journal de Physique I France*, Vol. 2, No. 12, pp. 2221-2229, Dec. 1992.

[48] B. Derrida, M. R. Evans, V. Hakim and V. Pasquier, "Exact solution of a 1D asymmetric exclusion model using a matrix formulation," *Journal of Physics A*, Vol. 26, No. 7, pp. 1493-1517, Apr. 1993.

[49] M. R. Evans, N. Rajewsky and E. R. Speer, "Exact solution of a cellular automaton for traffic," *Journal of Statistical Physics*, Vol. 95, Nos. 1/2, 1999.

[50] M. Haenggi, "Outage and throughput bounds for stochastic wireless networks," *IEEE International Symposium on Information Theory*, Sept. 2005

[51] S. P. Weber, J. G. Andrews, X. Yang and G. de Veciana, "Transmission capacity of wireless ad hoc networks with successive interference cancellation," *IEEE Transactions on Information Theory*, Vol. 53, No. 8, pp. 2799-2814, Aug. 2007.

[52] R. K. Ganti and M. Haenggi, "Dynamic Connectivity and Packet Propagation Delay in ALOHA Wireless Networks," *41st Asilomar Conference on Signals, Systems, and Computers*, Nov. 2007.

[53] A. Parmeggiani, T. Franosch and E. Frey, "The totally asymmetric simple exclusion process with Langmuir kinetics," *Physical Review. B, Condensed matter*, Vol. 70, Iss. 4, 2004.

[54] K. Qiu, X. Yang, W. Zhang, D. Sun and Y. Zhao, "Density profiles in the totally asymmetric exclusion processes with both local inhomogeneity and Langmuir kinetics," *Physica A: Statistical and Theoretical Physics*, Vol. 373, No. 1, pp. 1-10, Jan. 2007.

[55] A. El Gamal, J. Mammen, B. Prabhakar and D. Shah, "Throughput-Delay tradeoff in wireless network," *IEEE INFOCOM*, 2004.

[56] M. Xie and M. Haenggi, "Delay-Reliability Tradeoff in Wireless Networked Control Systems," in *Workshop on Networked Embedded Sensing and Control* Oct. 2005.

[57] Y. Li, M. Chiang, A. R. Calderbank and S. N. Diggavi, "Optimal rate-reliability-delay tradeoff in networks with composite links," *IEEE Transactions on Communications*, Vol. 57, No. 4, pp. 1-12, Apr. 2009.